SPONTANEOUS VORTEX PHASE AND PINNING IN FERROMAGNETIC-SUPERCONDUCTING SYSTEMS

A Dissertation

by

MOHAMMAD AMIN KAYALI

Submitted to the Office of Graduate Studies of
Texas A&M University
in partial fulfillment of the requirements for the degree of

DOCTOR OF PHILOSOPHY

May 2004

Major Subject: Physics

SPONTANEOUS VORTEX PHASE AND PINNING IN FERROMAGNETIC-SUPERCONDUCTING SYSTEMS

A Dissertation

by

MOHAMMAD AMIN KAYALI

Submitted to Texas A&M University
in partial fulfillment of the requirements
for the degree of

DOCTOR OF PHILOSOPHY

Approved as to style and content by:

Valery L. Pokrovsky (Chair of Committee)	
Donald G. Naugle (Member)	Wayne M. Saslow (Member)
Stephen A. Fulling (Member)	Edward S. Fry (Head of Department)

May 2004

Major Subject: Physics

ABSTRACT

Spontaneous Vortex Phase and Pinning in
Ferromagnetic-Superconducting Systems. (May 2004)
Mohammad Amin Kayali, M.S., Texas A&M University
Chair of Advisory Committee: Dr. Valery L. Pokrovsky

Heterogeneous ferromagnetic-superconducting systems such as a regular array of ferromagnetic nano dots deposited on the top of a superconducting thin film have attracted many research teams both experimental and theoretical. The interest in these systems does not only stem from being good candidates for technological applications, but also because they represent a new class of physical systems where two competing order parameters can coexist. This work focuses on the theoretical aspects of these systems by studying the static and dynamics of few model systems. In the first part, the static properties of a superconducting thin film interacting with a ferromagnetic texture are considered within the London approximation. In particular, the ferromagnetic textures considered here are a circular dot of submicrometer size with in-plane magnetization, an elliptical dot magnetized in the direction perpendicular to the superconductor, and a ferromagnetic dot magnetized in the direction normal to the superconducting film and containing non magnetic cavities. I also consider the interaction of vortices in the superconductor with a ferromagnetic columnar defect which penetrate the supercondcting film. In each case the vector potential and magnetic field of the ferromagnet in the presence of the superconductor are calculated. Afterward the presence of vortices in the superconductor is assumed and the energy of vortex-texture system is found. The pinning potential and force supplied by the texture are then derived from the energy of interaction between the ferromagnet

and superconductor. I show that if the magnetization of the ferromagnet exceeds a critical value then vortices are spontaneously created in the ground state of the system. Such spontaneous creation of vortices is possible mostly in a close vicinity of the superconducting transition temperature T_s. For every case, the threshold value of the magnetization at which vortices start to be spontaneously created in the SC is calculated as a function of the parameters of the texture geometry. The phase diagrams for transitions from vortexless regime to regimes with one or more vortices are determined for all cases.

In the second problem, the transport properties of a ferromagnetic superconducting bilayer with alternating magnetization and vortex density are studied within a phenomenological model. I show that pinning forces do not appear for continuous distribution of vortices, so a discrete model for the bilayer system is constructed. Afterward, I calculate the pinning forces acting on vortices and antivortices resulting from highly inhomogeneous distribution of flux lines and prove that this system has strong transport anisotropy. In the absence of random pinning, the system displays a finite resistance for the current in the direction perpendicular to the domains while its resistance vanishes for the parallel current. The transport anisotropy strongly depends on temperature. I study this dependence and show that the ratio of parallel to perpendicular critical current is largest close to the superconducting transition temperature T_s and the vortex disappearance temperature T_v while it has a minimum in between them.

To My Parents, Family, Brothers and Sisters.

ACKNOWLEDGMENTS

The work presented in here would not have been possible without the help and support of many people. Therefore, I would like to take this opportunity to specially thank my advisor Dr. Valery L. Pokrovsky for his support, paitience and encouragements over the last five years. I would like to thank him not only for teaching me new concepts and introducing me to the fascinating world of condensed matter physics, but also for sharing with me his comprehensive understanding of physics in general. I also would like to thank my committee members, Dr. Wayne Saslow, Dr. Donald Naugle and Dr. Stephen Fulling, for their help, support, and the efforts they made to make this happen. Special thanks goes to my colleagues and collaborators, in particular I would like to thank Dr. Nizar Hamdan, Dr. Zaid Al-Amir, Dr. Wayne Saslow Dr. Vladimir Kogan, Dr. Igor Lyuksyutov, Dr. Serkan Erdin, Mr. Nicolai Sinitsyn and Dr. Arman Kirakosyan and many others for numerous discussions and valuable contributions. I am also grateful to my parents, my siblings, my wife Minawar, and our kids Romina, Farouk and Hind for their support and love and for believing in me.

TABLE OF CONTENTS

LIST OF FIGURES

FIGURE Page

CHAPTER I

INTRODUCTION

Dissipation in type two superconductors (SC) is due to phase slippage, which may arise due to the motion of vortices or the existence of phase-slip centers or lines. To enhance the critical current of a superconductor the motion of vortices must be stopped; this occurs by what is known as vortex pinning. Therefore, it is very important both theoretically and experimentally to understand the pinning mechanisms and how to optimize pinning. In principle, most lattice defects create pinning potentials for flux lines in superconductors. The defects are either native to the superconductor's lattice or artificially introduced. Artificial pinning sites such as random columnar defects are typically created by heavy-ion irradiation [1]. The heavy-ion irradiation method creates random pinning centers. Vortex pinning and transport properties of superconductors with random pinning centers were well studied and thoroughly reviewed in [2]. It was shown later that flux pinning can be enhanced by employing a regular array of defects in the superconductor. Magnetization, critical current and resistivity measurements performed on systems consisting of a superconductor covered by a regular array of artificially created structural defects displayed commensurability effects [3], [4] that were not observed in systems with random pinning. The commensurability between the flux lattice and the defect array resulted in higher critical currents. Of particular interest are the results of the experiment by Martinoli *et.al* [5] who studied the transport properties of a SC film of periodically modulated thickness and observed oscillations of the critical current as a function of the applied magnetic field. It is worth mentioning that pinning in superconductors with artificial colum-

---

The journal model is Physical Review Letters.

nar defects such as those created by the heavy-ion irradiation is due to the multiply connected topology of the superconductor. The origin of pinning in superconductors with multiply connected topologies pertains to the variations in the effective value of the Ginzburg-Landau parameter $\kappa = \frac{\lambda}{\xi}$ in the neighborhood of the defect.

In recent years the interest in heterogeneous ferromagnetic-superconducting systems (HFSS) has grown rapidly due to the preliminary experimental data which showed improved pinning strength in these systems. These systems typically consist of a superconductor placed in close proximity with a ferromagnet (FM). A thin layer of insulator oxide is sandwiched between the FM and SC to prevent proximity effects and spin diffusion, which both tend to destroy superconductivity. The interest in HFSS is motivated not only because of their technological importance but also for being a new class of physical systems in which two competing order parameters may coexist and possibly enhance one another. Several experimental groups [6], [7], [8], [9], [10] have investigated pinning in HFSS and found appreciable increases in the critical current. In most experiments, the superconductor is a continuous two dimensional sheet covered by a regular array of ferromagnetic dots. Each dot has a radius of the order of the SC penetration depth λ and is magnetized in a direction either parallel or perpendicular to the SC. It is important to realize that pinning in HFSS does not appear due to the multiply connected topology, as occurs when the defect is established in the SC. It is rather due to the strongly inhomogeneous distribution of the magnetic field generated by the magnetic structure.

In 1957, Ginzburg [11] argued that superconductivity and ferromagnetism may coexist in systems of dimension $D \leq 2$ due to the large critical field of low-dimensional superconductors. However, proximity effects and spin diffusion pose serious problem for the coexistence of the two phenomena. To solve this problem, Lyuksyutov and Pokrovsky [12], [13] proposed to separate the ferromagnet and superconductor by

inserting a thin layer of insulator oxide, which supresses proximity effects. The FM and SC are now electronically separated; therefore, they interact solely via their magnetic fields without destroying one another's order parameter. Different realizations of HFSS were studied both experimentally and theoretically. Special consideration was given to the system of a superconducting thin film covered by a regular array of ferromagnetic nano-dots [6], [7], [8], [9], [10]. Such systems are usually prepared using electron-beam lithography and lift-off techniques [14]. The dots are magnetized either in the direction parallel or perpendicular to the SC film. These studies reported the observation of commensurability effects in these systems. The essence of these effects is that the dot array spontaneously creates vortices in the SC, which in turn will be pinned by the dots. Commensurability effects appear when the density of vortices in the SC is a fractional number of the density of dots in the FM.

Theoretically, many HFSS systems with different magnetization distributions were studied [15], [16], [17], [18], [19], [20], [21], [22]. Almost a decade ago [17], Marmorkos *et.al.* studied the interaction between a ferromagnetic disk embedded in a bulk superconductor and showed that the disk generates several vortices in the SC. Their approach was to numerically solve the nonlinear Ginzburg-Landau equation with appropriate boundary conditions after taking into account the magnetic vector potential generated by the dot. In another work [21], Sasik and Hwa considered a system consisting of a superconducting thin film covered by magnetic dots. They assumed the dots to be magnetized in a direction perpendicular to the SC film. They also simplified the problem by ignoring the real geometry of the dots by replacing them by point dipoles. This is the main drawback of their work since the geometry of the FM is of great importance in the study of the statics and dynamics of any HFSS. They were able to show that, in the absence of an external magnetic field, a spontaneous creation of superconducting vortices can take place if the stray mag-

netic field generated by the dot exceeds the field necessary to create vortices in the superconductor.

In [20], Erdin, *et.al.* studied the ground state of a ferromagnetic-superconducting bilayer (FSB). They found that the homogeneous state, which is characterized by a magnetization directed perpendicular to the FM, can be unstable with respect to the creation of vortices in the SC. They showed that the weak interaction between the created vortices makes the structure with alternating domains an energy favorable ground state. They also considered the possibility of other structures, showing that the structure with alternating stripe domains costs less energy than other structures. Therefore, they speculated that a strong transport anisotropy can be viewed as an indirect observation of the stripe domain structure in the FSB.

Motivated by the current theoretical and experimental interest in the static and dynamical phases of the HFSS, I present theoretical studies of static and transport properties of some HFSS. Chapter two is divided into five sections and is entirely devoted to the general formulation and their static properties of HFSS. Section one presents a general formulation for a system consisting of a SC film in close proximity with a FM texture. Section two studies the interaction between a SC thin film and a circular FM dot of radius $R \gg \xi$ whose magnetization vector lies in its plane. I calculate the magnetic vector potential and field generated by the dot in the presence of the SC. Above a threshold value of the dot's magnetization, the interaction between the dot and the SC makes the spontaneous creation of vortex-antivortex pairs energy favorable. The creation of one or more vortex-antivortex pairs is studied and their equilibrium distribution is found.

In section three, I investigate the interaction between a SC thin film and an elliptical FM dot whose magnetization is normal to the plane of the superconductor. After finding the magnetic field and current distributions, I calculate the energy of

interaction between the dot and the SC. Above the threshold value of the dot's magnetization, spontaneous creation of vortices is energy favorable; therefore, I calculate the phase diagram of the system. The effect of geometry and shape anisotropy on the pinning potential and creation of vortices is considered by comparing the results for the elliptical dot with those for a circular one. I show that elliptical dots are more effective for pinning and are more likely to spontaneously create vortices in superconductors. The interaction of SC vortices with a FM annulus whose magnetization is perpendicular to the plane of the superconductor is studied in section four. I calculate the pinning forces exerted by the annulus on vortices in the superconductor. In equilibrium, the vortex sits under the annular region on a circle of radius ρ_0 that depends on the radii and magnetization per unit area of the annulus, and on the SC penetration depth λ. In section five I focus on pinning and spontaneous vortex creation by a ferromagnetic rod which penetrates the superconductor. The pinning potential when the rod magnetization is zero reduces to the value calculated by Mkrtchyan and Schmidt [23], which states that the pinning force on the vortex vanishes if the center of the vortex is trapped inside the columnar defect. However, for non-zero magnetization the pinning potential is strongly enhanced and the pinning force does not vanish anywhere near the rod. In the absence of externally induced vortices, the FM rod could spontaneously create vortices in the SC when its magnetization is more than a critical value.

Chapter three studies the transport properties of the FSB. Because pinning forces do not appear in the continuous model developed in [20], a discrete model for the FSB must be constructed. The interaction of the FM with the SC makes the pinning forces acting on the vortices and antivortices in the direction parallel to the domain much smaller than its value in the direction perpendicular to the domains. Therefore, the critical current will depend on the angle at which the transport current is applied.

I show that the system displays a finite resistance to the current when the current is applied perpendicular to the domains and is superconducting when it is parallel. I show that the transport anisotropy is strongest at temperatures close to the SC transition temperature T_s and the vortex disappearance temperature T_v. Finally, these results are summarized in chapter four and a glossary of acronyms is given in chapter five.

CHAPTER II

STATIC PROPERTIES OF HETEROGENEOUS FERROMAGNETIC-SUPERCONDUCTING SYSTEMS

In this chapter I focus on the static properties of heterogeneous ferromagnetic superconducting systems. The inhomogeneous distribution of magnetization produces a magnetic field in space which modifies the screening currents in the superconductor. In turn the superconductor generates a magnetic field that interacts with the magnetic structure, so the problem must be solved self consistently. Here, I am mainly consider systems for which the FM structure thickness and all other thicknesses are much less than the penetration depth of the superconductor. Therefore, it is sufficient to employ the London approximation to study the static properties of these systems. After introducing the London approximation, I present studies of three model systems. In particular, I first study the static properties of a superconducting thin film covered by a circular ferromagnetic dot whose magnetization is directed parallel to the plane of the SC. In the second example, the dot is replaced by an elliptical ferromagnetic dot whose magnetization is directed along the normal to the SC film. I study the static properties of this system and compare it to the case of circular dot. I also study pinning and spontaneous vortex creation by an FM annulus on the top of a SC film. Finally, I investigate the interaction between vortices in a SC film with a ferromagnetic rod magnetized along its symmetry axis and perpendicularly penetrating the superconductor.

A. London Approximation and HFSS

Let the SC thin film be in the xy-plane and an infinitely thin ferromagnetic texture is placed on the top of it at a distance $a_0 \ll D \sim \xi$, where a_0 is an atomic dimension

and ξ is the SC coherence length. Thus the interaction between the ferromagnet and superconductor occurs via their magnetic fields, the theory to calculate the total magnetic field and screening currents is developed here. Let the magnetization distribution of the FM texture be $\mathbf{M}(\mathbf{r})$. The total magnetic field $\mathbf{B} = \mathbf{B}^s + \mathbf{B}^m$ is derived from the total vector potential $\mathbf{A} = \mathbf{A}^s + \mathbf{A}^m$, where the superscripts (s) and (m) refer to the superconducting and ferromagnetic parts respectively. The total vector potential is governed by Maxwell's equation

$$\nabla \times (\nabla \times \mathbf{A}) = \frac{4\pi}{c}(\mathbf{J}_s + \mathbf{J}_m) \tag{2.1}$$

and

$$\mathbf{J}^s = \frac{n_s \hbar e}{2m_s}(\nabla\varphi - \frac{4\pi e}{hc}\mathbf{A}) \tag{2.2}$$

$$\mathbf{J}^m = c\nabla \times \mathbf{M}. \tag{2.3}$$

Here $\hbar$ is Planck constant, c is the speed of light, n_s is the superconducting electron density, m_s and e are their mass and charge respectively, and φ is the phase of the SC order parameter. For an SC thin film of thickness d_s, the effective penetration depth λ is defined in terms of the London penetration depth λ_L as

$$\lambda = \frac{\lambda_L^2}{d_s} \tag{2.4}$$

with

$$\lambda_L = \sqrt{\frac{m_e c^2}{4\pi n_s e^2}} \tag{2.5}$$

The presence of N-vortex in the superconductor, the phase gradient of the order

parameter is

$$\nabla\varphi = \sum_{i=1}^{N} \nu_i \frac{\hat{z} \times (\mathbf{r} - \mathbf{r}_i)}{|\mathbf{r} - \mathbf{r}_i|^2} \tag{2.6}$$

where ν_i and ρ_i are the vorticity and the location of the i-th vortex. Use of the superposition principle permits separation of the vortex part of the vector potential from that of the ferromagnet. The solution for the vortex part gives the Pearl solution for the vortex vector potential [24],[25],[26]

$$\mathbf{A}_v(\mathbf{r} - \mathbf{r}_0, z) = \frac{\phi_0}{2\pi} \sum_{i=1}^{N} \nu_i \frac{\hat{z} \times (\mathbf{r} - \mathbf{r}_i)}{|\mathbf{r} - \mathbf{r}_i|} \int_0^\infty \frac{J_1(q|\mathbf{r} - \mathbf{r}_i|)e^{-q|z|}}{1 + 2\lambda q} dq \tag{2.7}$$

where $q = |\mathbf{q}|$ is the amplitude of the 2D wave vector. The FM part of the vector potential is the solution of the following equation

$$\nabla \times (\nabla \times \mathbf{A}) = -\frac{1}{\lambda}\mathbf{A}\delta(z) + 4\pi\nabla \times [\mathbf{m}(\rho)\delta(z)] \tag{2.8}$$

where $\mathbf{m}(\rho)$ is the two-dimensional magnetization of the texture.

The two-dimensional magnetization can be decomposed into three parts. The first part is perpendicular to the SC film m^z and the second part $m^{||}$ is directed along the radial vector $\hat{\rho}$. The remaining part $m^{\perp}$ is directed along the unit vector $\hat{\rho} \times \hat{z}$ that is perpendicular to the plane spanned by $\hat{\rho}$ and $\hat{z}$. The solution of Eq.(2.8) is easily obtained using Fourier transform defined for any function $f(\mathbf{x})$ as

$$f(\mathbf{x}) = \frac{1}{(2\pi)^3} \int f_{\mathbf{k}} e^{-\imath \mathbf{k}\cdot\mathbf{x}} d^3\mathbf{k} \tag{2.9}$$

where $\mathbf{k} = (\mathbf{q}, k_z)$ is the $3D$ wave vector and $f_{\mathbf{k}}$ is the Fourier kernel. The solution of (2.8) can be represented by its Fourier kernel components [16] as:

$$A^{||}_{m\mathbf{k}} = -\frac{4\pi\imath m^{\perp}_{\mathbf{q}}}{k_z} e^{\imath k_z D} \tag{2.10}$$

$$A^{\perp}_{m\mathbf{k}} = -\frac{a^{\perp}_{\mathbf{q}}}{\lambda k^2} + \frac{4\pi\imath(k_z m^{||}_{\mathbf{q}} - q m_{\mathbf{q}z})}{k^2} e^{\imath k_z D} \tag{2.11}$$

where $\mathbf{a}_{m\mathbf{q}}$ is the Fourier transform of the vector potential at the SC film. Here $a^{||}_{m\mathbf{q}} = 0$ while

$$a^{\perp}_{\mathbf{q}} = -\frac{4\pi\lambda q(k_z m^{||}_{\mathbf{q}} - q m_{\mathbf{q}z})}{1 + 2\lambda q} e^{-qD} \tag{2.12}$$

Note that $A^{||}_{m\mathbf{k}}$ does not contain any information about the superconductor, so it is not affected by the presence of the superconductor in contrast to $A^{\perp}_{m\mathbf{k}}$. Now, the total magnetic field and energy of the HFSS can be calculated. The magnetic field's components can be calculated from the vector potential $\mathbf{A}$ from its definition $\mathbf{B} = \nabla \times \mathbf{A}$. This can be written in Fourier space as follows

$$B^{z}_{m\mathbf{k}} = \imath q A^{\perp}_{m\mathbf{k}}, \quad B^{||}_{m\mathbf{k}} = -\imath k_z A^{\perp}_{m\mathbf{k}}, \quad B^{\perp}_{m\mathbf{k}} = \imath k_z A^{||}_{m\mathbf{k}}. \tag{2.13}$$

The total energy of the HFSS is the sum of the vortex self energy U_{sv}, the vortex-vortex interaction U_{vv}, the energy of interaction between the ferromagnet and vortices U_{mv} and the magnet self interaction U_{mm}. If there are N vortices in the superconductor, then their total vector potential is the superposition of their individual potentials. This can be written in Fourier representation as follows

$$A_{v\mathbf{k}} = \frac{-2\imath\phi_0(\hat{z} \times \hat{q})F(\mathbf{q})}{k^2(1 + 2\lambda q)} \tag{2.14}$$

where $F(\mathbf{q}) = \sum_{j=1}^{N} \nu_j e^{\imath \mathbf{q} r_j}$ with r_j is the position of the j-th vortex and ν_j is its vorticity. The total energy of the HFSS can be written as

$$U = \int \left[\frac{\mathbf{B}^2}{8\pi} + \frac{m_s n_s v_s^2}{2} - \mathbf{M} \cdot \mathbf{B} \right] d^3x \tag{2.15}$$

where v_s is the superconducting carrier velocity defined as

$$v_s = \frac{\hbar}{2m_e}\nabla\varphi \tag{2.16}$$

The terms in the square bracket are as follows: the first term is the magnetic field energy, the second term is the kinetic energy due to the SC electrons and the last term is the Zeeman interaction term. Using Maxwell's equation $\nabla \times \mathbf{B} = (4\pi/c)\mathbf{J}$ with $\mathbf{B} = \nabla \times \mathbf{A}$, and integrating by parts then the magnetic energy can be rewritten as

$$\int \frac{\mathbf{B}^2}{8\pi} d^3x = \int \frac{\mathbf{J}\cdot\mathbf{A}}{2c} d^3x \tag{2.17}$$

This equation is gauge invariant because the total current is conserved ($\nabla \cdot \mathbf{J} = 0$). I have omitted a surface term which arises from integration by parts. This is possible only because the vector potential and the currents decrease rapidly as $\mathbf{r}$ approaches infinity. The part due to the magnetic texture may be transformed to

$$\int \frac{\mathbf{J}_m \cdot \mathbf{A}}{2c} d^3x = \frac{1}{2}\int \mathbf{M}\cdot\mathbf{B} d^3x \tag{2.18}$$

Therefore, I rewrite (2.15) as

$$U = \int \left[\frac{n_s\hbar^2}{8m_s}(\nabla\varphi)^2 - \frac{n_s\hbar e}{4m_s c}\nabla\varphi\cdot\mathbf{A} - \frac{\mathbf{M}\cdot\mathbf{B}}{2}\right] d^3x \tag{2.19}$$

For the case when the SC and the FM thicknesses are infinitesimally small. Hence the total energy given by (2.19) must be modified by taking the 3D density of superconducting electrons in the SC film to be $n_s(\mathbf{r}) = n_s(\rho)\delta(z)$ and the 3D magnetization to be expressed in terms of the 2D magnetization $\mathbf{m}(\rho)$ of the FM as $\mathbf{M}(\mathbf{r}) = \mathbf{m}(\rho)\delta(z - D)$. In this case, the vortex self energy and the vortex-vortex

interaction can be written as:

$$U_v = \frac{n_s \hbar^2}{8 m_s} \int \nabla \varphi_{-\mathbf{q}} \cdot (\nabla \varphi_{\mathbf{q}} - \frac{2\pi}{\phi_0} \mathbf{a}_{v\mathbf{q}}) \frac{d^2 q}{4\pi^2} \tag{2.20}$$

The interaction energy between superconducting vortices and ferromagnet is

$$U_{mv} = -\frac{n_s \hbar e}{4 m_s c} \int \nabla \varphi_{-\mathbf{q}} \cdot \mathbf{a}_{m\mathbf{q}} \frac{d^2 q}{4\pi^2} - \frac{1}{2} \int \mathbf{m}_{-\mathbf{q}} \cdot b_{v\mathbf{q}} \frac{d^2 q}{4\pi^2} \tag{2.21}$$

The ferromagnet self interaction energy U_{mm} is

$$U_{mm} = -\frac{1}{2} \int \mathbf{m}_{-\mathbf{q}} \cdot b_{m\mathbf{q}} \frac{d^2 q}{4\pi^2} \tag{2.22}$$

where $b_{m\mathbf{q}}$ and $b_{v\mathbf{q}}$ used in Eq.(2.20)-(2.22) are the Fourier representation of the magnetic fields generated by the FM and the vortex evaluated at the surface of the superconductor. The total energy U is the sum $U = U_v + U_{mv} + U_{mm}$. This is a many variable function with its variables being the locations of the N vortices. Therefore, the distribution of vortices which minimizes the total energy of the system must be found. In most cases the total energy of the system is a very complex function of the locations of vortices. Hence the minimal energy configuration must be found numerically.

B. In-Plane Magnetized Dot

Martin *et.al.* [6] studied the properties of an SC thin film covered by a triangular array of submicrometer FM dots with in plane magnetization. They observed regular structures in the resistivity curve when plotted as a function of the magnetic field. They also reported the observation of resistivity minima at a constant field interval. Their measurements indicate an enhanced vortex pinning due to the presence of the dot array. In another experiment, [8] an array of ferromagnetic dots whose magneti-

zation is parallel to the SC film is placed on the top of a superconducting film. These measurements reflect a strong pinning of the flux lines by the dots. They also observed that in the absence of applied magnetic field a coupled vortex-antivortex pair appear under the dot with the vortex on one side of the dot and the antivortex on the other. Next I study vortex pinning and spontaneous creation of vortex-antivortex pairs theoretically. To study this system the problem is simplified by considering the action of a single FM dot on the SC film.

Let the SC film lie in the xy-plane top of it, at a distance $z = D$, with an infinitely thin FM dot whose radius is R and whose magnetization is pointing along the x-axis. Hence the magnetization can be rewritten as $\mathbf{M}(\mathbf{r}) = m_0\Theta(r-R)\delta(z-D)\hat{x}$ where m_0 is the two-dimensional magnetization of the dot, $\Theta(R-r)$ is the step function, and $\delta(z-D)$ is Dirac delta function. To study the interaction between the dot and the superconductor, I calculate the vector potential and magnetic field due to the dot in the presence of the superconductor. The Fourier transform of the dot's magnetization is

$$\mathbf{M}_\mathbf{k} = \frac{2\pi m_0 R}{q} J_1(qR) e^{\imath k_z D}\hat{x} \tag{2.23}$$

where $J_n(x)$ is the n-th order Bessel function. The magnetization (2.23) can be decomposed into $M^{\perp}_\mathbf{k}$ and $M^{||}_\mathbf{k}$ such as

$$\mathbf{M}^{\perp}_\mathbf{k} = -\frac{2\pi m_0 R}{q} J_1(qR)\sin(\phi_q) e^{\imath k_z D} \tag{2.24}$$

$$\mathbf{M}^{||}_\mathbf{k} = \frac{2\pi m_0 R}{q} J_1(qR)\cos(\phi_q) e^{\imath k_z D} \tag{2.25}$$

where ϕ_q is the azimuthal angle in the wave vector space spanned by $(\mathbf{q}, k_z)$. Now, with the results (2.24) and (2.25) combined with equations (2.10) and (2.11), the

vector potential due to the dot in the presence of the superconductor is

$$A^{\perp}_{m\mathbf{k}} = \frac{8\pi^2 m_0 R}{k_z^2+q^2} J_1(qR)\cos(\phi_q)\left(\frac{\imath k_z e^{\imath k_z D}}{q} + \frac{e^{-qD}}{1+2\lambda q}\right) \tag{2.26}$$

$$A^{||}_{m\mathbf{k}} = \frac{8\pi^2 \imath m_0 R}{k_z q} J_1(qR)\sin(\phi_q) e^{\imath k_z D} \tag{2.27}$$

The Fourier transform of the dot's vector potential at the surface of the superconductor is

$$a^{\perp}_{m\mathbf{q}} = -\frac{8\pi^2 m_0 \lambda R}{1+2\lambda q} J_1(qR)\cos(\phi_q) e^{-qD} \tag{2.28}$$

The magnetic field has three components $B^{||}$, $B^{\perp}$ and B^z; of particular interest to us here are $B^{||}$ and B^z. The inverse Fourier transforms of $B^{||}_{m\mathbf{k}} = -\imath k_z A^{\perp}_{m\mathbf{k}}$ and $B^z_{m\mathbf{k}} = \imath q A^{\perp}_{m\mathbf{k}}$ are

$$\begin{aligned} B^z_m(\rho,\phi,z) = 2\pi m_0 R\cos(\phi)\int_0^{\infty} qJ_1(qR)J_1(q\rho)\times \\ \left(\frac{e^{-q(|z|+D)}}{1+2\lambda q} - sign(D-z)e^{-q|D-z|}\right)dq \end{aligned} \tag{2.29}$$

$$\begin{aligned} B^{\rho}_m(\rho,\phi,z) = 2\pi m_0 R\cos(\phi)\int_0^{\infty} qJ_1(qR)J_0(q\rho)\times \\ \left(2\delta(z-D) - qe^{-q|D-z|} - \frac{qe^{-q(|z|+D)}}{1+2\lambda q}sign(z)\right) \end{aligned} \tag{2.30}$$

where the $sign(x)$ is $+1$ for $x > 0$ and -1 for $x < 0$. Note that B^{ρ}_m and B^z_m both have discontinuities at $z = 0$ and $z = D$. Therefore, extra care is needed to calculate the field components at the SC surface.

Before discussion of the energy of the system I analyze the behavior of the magnetic field of the dot at the surface of the SC film. The magnetic field generated by the magnetic dot in the absence of the superconductor is equivalent to the field of

a ring of radius R with a $\cos(\phi)$ magnetic charge distribution. The z-component of the dot's magnetic field vanishes at the center of the dot then it increases to reach a maximum at $\rho = R$. At large distances $\rho > R$, it decays as $1/\rho^3$. The component B_m^ρ is maximum at $\rho = 0$. The magnetic field of the dot has all three components but only B_m^z and B_m^ρ are of interest for two reasons. First, B_m^ϕ does not contain any information about the superconductor, it is exactly equal to its value in the absence of the SC. Second, the vortex's magnetic field has only B_v^ρ and B_v^z components, so it is not affected by B_m^ϕ.

Both B_m^z and B_m^ρ have maxima at $\phi = 0$ and minimum at $\phi = \pi$. If flux lines are to appear in the SC due to the field of the dot, then a vortex-antivortex pair would appear with the vortex at some $\rho = \rho_0$ and another at $\rho = -\rho_0$, with ρ_0 to be determined.

The total energy for a system of magnetic dot with in-plane magnetization interacting with N single quanta flux lines is

$$U_N = N\epsilon_0 \ln(\frac{\lambda}{\xi}) + \frac{1}{2}\sum_{i\neq j}^{N} \nu_i \nu_j \epsilon_{vv}(|\rho_i - \rho_j|) + \sum_{i=1}^{N} \nu_i \epsilon_{mv}(\rho_i) \tag{2.31}$$

where $\nu_i = +1$ for a vortex and $\nu_i = -1$ for antivortex while

$$\epsilon_0 = \frac{\phi_0^2}{16\pi^2\lambda} \tag{2.32}$$

Here ϵ_{vv} is the vortex-vortex interaction which can be expressed in terms of Neumann's function H_0 and the Struve function Y_0 [27] as

$$\epsilon_{vv}(|\rho_i - \rho_j|) = \frac{\epsilon_0}{\pi}\left(H_0(\frac{|\rho_i - \rho_j|}{2\lambda}) - Y_0(\frac{|\rho_i - \rho_j|}{2\lambda})\right) \tag{2.33}$$

The interaction energy between a flux line and the magnetic dot can be calculated from (2.28) together with the phase gradient and magnetic field due to the flux line

at ρ_i. It is

$$\epsilon_{mv}(\rho_i) = -\epsilon_m R\cos(\phi_i)\int_0^\infty \frac{J_1(qR)J_1(q\rho_0)}{1+2\lambda q}dq \tag{2.34}$$

with ϵ_m is energy scale for the FM-SC interaction and is defined as

$$\epsilon_m = m_0\phi_0 \tag{2.35}$$

If the SC has only one vortex-antivortex pair then it is logical to assume that the vortex and antivortex will be located on the x-axis since the magnetic field is strongest on the x-axis with respect to its angular distribution. Therefore, the case when the vortex is at $x = -\rho_0$ and the antivortex at $x = +\rho_0$ is studied. The total energy for a vortex-antivortex pair coupled to a magnetic dot is

$$\begin{aligned} E_{N=2} &= 2\epsilon_0\ln(\frac{\lambda}{\xi}) - 4\epsilon_0\lambda\int_0^\infty \frac{J_0(2q\rho_0)}{1+2\lambda q}dq \\ &\quad -2\epsilon_m R\int_0^\infty \frac{J_1(qR)J_1(q\rho_0)}{1+2\lambda q}dq + E_0 \end{aligned} \tag{2.36}$$

The first and second terms in (2.36) represent the energy of the flux lines without the magnetic dot. The third term is the interaction energy between the flux lines and the magnetic dot, and E_0 is the magnetic dot self interaction energy. Now consider the ratio δ_m between the two energy scale in the system

$$\delta_m = \frac{m_0\phi_0}{\epsilon_0} \tag{2.37}$$

Note that the larger the values of δ_m are, the more favorable it is to have vortex-antivortex pairs in the SC. Using (2.32) and putting $m_0 = n_m d_m g\mu_B S$ then δ_m can be written in terms of the characteristics quantities of the SC and FM films as follows

$$\delta_m = gS\frac{n_m d_m}{n_s(T)d_s} \tag{2.38}$$

where g is Lande factor and $mu_B = \hbar e/2m_e c$ is Bohr's magneton. Here S is the elementary spin of the FM, while n_m and n_s are the electronic density for the FM and SC respectively with d_m the thickness of the FM film and similarly d_s that for the SC. Note that, close to the superconducting transition temperature T_s the SC electrons density becomes very small making δ_m very large.

The energy (2.36) is numerically minimized with respect to ρ_0 to find that $E_{N=2}$ is a minimum at $\rho_0 = R$. The presence of the vortex-antivortex pair changes the energy of the system by an amount Δ_1 given by

$$\Delta_1 = 2\epsilon_0 \ln(\frac{\lambda}{\xi}) - 4\epsilon_0\lambda \int_0^\infty \frac{J_0(2qR)}{1+2\lambda q} dq - 2m_0\phi_0 R \int_0^\infty \frac{J_1(qR)J_1(qR)}{1+2\lambda q} dq \qquad (2.39)$$

The creation of a vortex-antivortex pair is energy favorable if the energy of the overall system is lowered by such process. Let us redefine Δ_1 by dividing both sides of (2.39) by ϵ_0 to obtain a dimensionless function of the two variables R/λ and δ_m. The curve $\Delta_1 = 0$ depicted in Fig.1 separates between a regime without magnetic flux in the SC from another with one vortex-antivortex pair. The region above the curve represents a phase with one vortex-antivortex pair while that under the curve refers to a system without any flux line.

Next, I consider the creation of two vortex-antivortex pairs coupled to the FM dot. In this case extra caution in handling the energy's angular dependence must be used. The results above show that the first pair appears with the vortex and antivortex situated along the x-axis with their centers under the edge of the dot. For two vortex-antivortex pairs, two vortices will appear on one side of the dot and two antivortices will be on the other side. Moreover, because like vortices repel one another, there are two possibilities. The first is that the two vortices will be on radial line on one side of the dot on the x-axis, and antivortices on radial line on the other side of the dot. The second is that the two vortices will be symmetrically off the

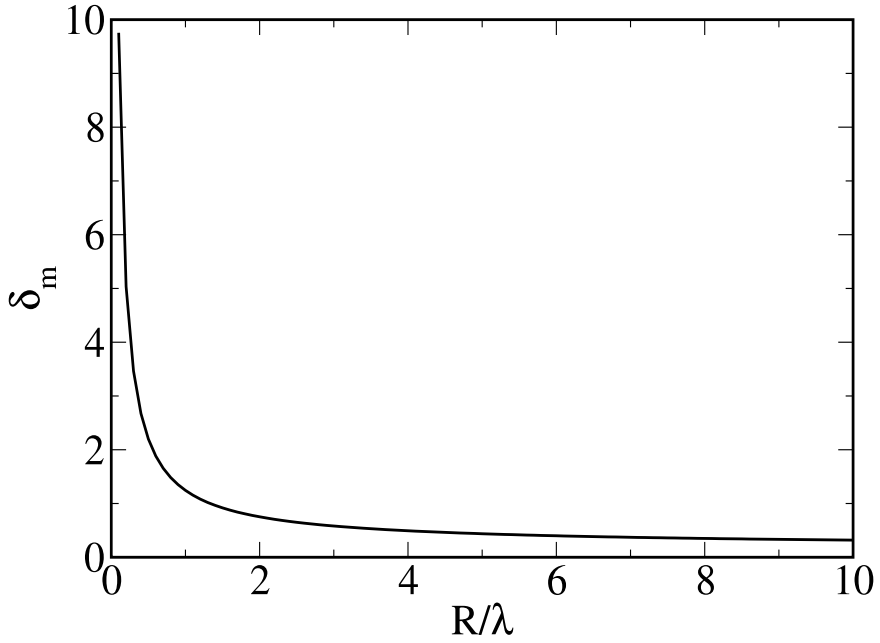

Fig. 1. Phase diagram for one vortex-antivortex pair creation by a magnetic dot with in-plane magnetization.

x-axis as shown in Fig.2.

To study the creation of two pairs, the flux form factor $F(q)$ must be modified, and then the energy of the system recalculated. For the purpose of calculating the total energy of the system I assume that the center of each flux line is at $\rho = \rho_0$ from the origin chosen to be under the center of the dot. The energy of a magnetic dot coupled to two vortex-antivortex pairs is not only dependent on ρ_0 but also depends on the angle between the flux line and the x-axis θ; therefore, the energy of the system must be minimized with respect to both ρ_0 and θ. The numerical simulations show that $\rho_0 = R$ is still the minimum, so I set ρ_0 equal to R and minimize the energy with respect to θ. I find the minimum energy configuration occurs for $\rho_0 = R$ and $13^\circ < \theta < 17^\circ$, as illustrated in Fig.3.

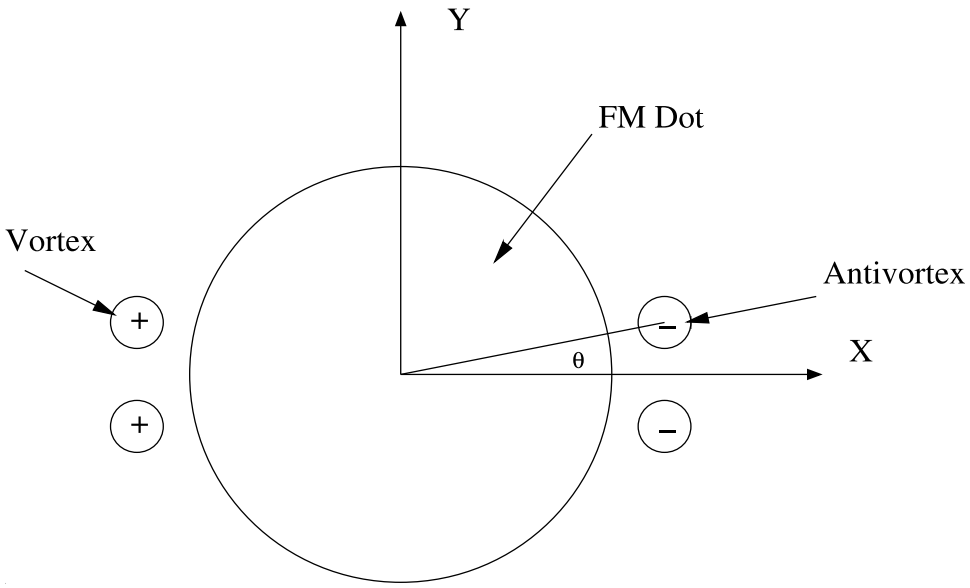

Fig. 2. Illustration of two vortex-antivortex pairs in a superconducting thin film coupled to a ferromagnetic dot with in-plane magnetization.

C. Elliptic Dot and Shape Anisotropy Effect on Pinning.

In this section, I present a theoretical study of the interaction between vortices in a superconducting thin film and elliptic ferromagnetic dots (EMD). I will also study the effect of shape anisotropy of the dot on pinning in this HFSS. The study of the interaction between elliptic dots and superconductivity is interesting since its results when the dot's eccentricity $\mathcal{E}$ is zero, corresponding to those known results for circular dots. Another interesting limit is when $\mathcal{E} \to 1$ which mimics a system of long magnetic stripe domains interacting with an SC film.

To begin, let us consider a superconducting thin film of thickness d_s, whose coherence length is ξ and its penetration depth is λ in the xy-plane. We place on the top of it at a distance $D \ll \lambda$ an elliptical ferromagnetic dot of major axis R_1 and minor axis R_2. Let the dot magnetization $\mathbf{M}$ be directed along the z-axis, so the

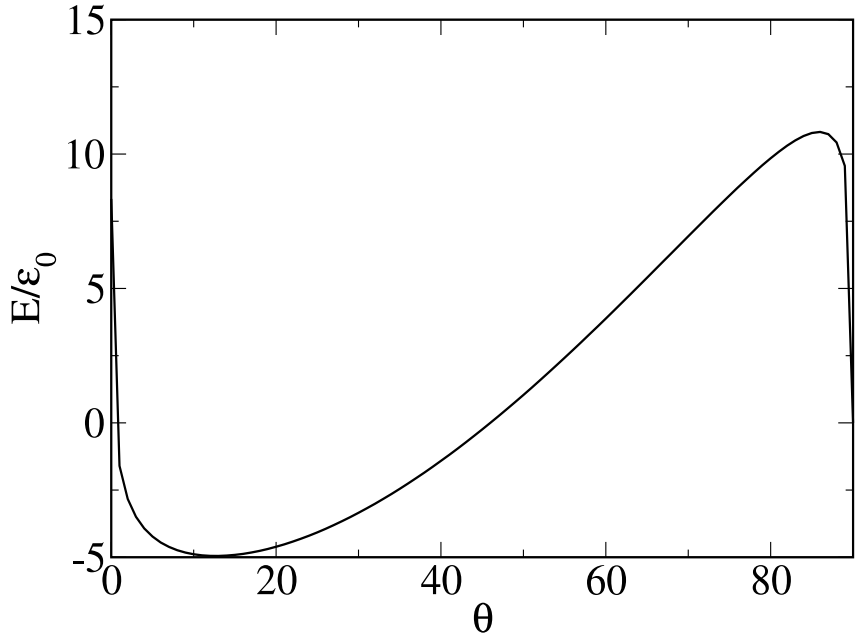

Fig. 3. The angular dependence of the energy of two vortex-antivortex pairs created by a magnetic dot with in-plane magnetization.

magnetization distribution can be written as

$$\mathbf{M}(x,y,z) = m_0\Theta(1-\frac{x^2}{R_1^2}-\frac{y^2}{R_2^2})\delta(z-D)\hat{z} \tag{2.40}$$

where m_0, is the two-dimensional magnetization, $\Theta(r)$ is the step function and $\delta(r)$ is Dirac delta function as before.

In the presence of the superconductor the magnetic vector potential $\mathbf{A_m}$ of the dot satisfies the London-Maxwell equation. Using the Coulomb gauge $\nabla \cdot \mathbf{A_m} = \mathbf{0}$, and the Fourier representation for $\mathbf{A}_m$, I find

$$\tilde{\mathbf{A}}_m(\mathbf{K}) = \frac{-8\pi^2\imath m_0 R_1 R_2 J_1\left(G(k_x,k_y)\right)}{G(k_x,k_y)\left(k_z^2+q^2\right)}\left(e^{\imath k_z D}-\frac{e^{-qD}}{1+2\lambda q}\right)\hat{z}\times\mathbf{q} \tag{2.41}$$

where $\tilde{\mathbf{A}}_m$ is the magnetic dot vector potential in Fourier representation and $\mathbf{q} =$

$k_x\hat{x} + k_y\hat{y}$ is Fourier wave vector in the plane of the SC. The function $J_n(r)$ is the n-th order Bessel Function, and $G(k_x, k_y) = \sqrt{R_1^2 k_x^2 + R_2^2 k_y^2}$. By using $\mathbf{B} = \nabla \times \mathbf{A}$, the components of the dot's magnetic field are given by

$$B_{mz} = m_0 R_1 R_2 \int \frac{q J_1(G(k_x, k_y)) Z(k_x, k_y)}{G(k_x, k_y)} e^{-\imath(k_x x + k_y y)} d^2 q \tag{2.42}$$

$$B_{mj} = \imath m_0 R_1 R_2 \int \frac{k_j J_1(G(k_x, k_y)) W(k_x, k_y)}{G(k_x, k_y)} e^{-\imath(k_x x + k_y y)} d^2 q \tag{2.43}$$

where $j = x, y$, with $Z(k_x, k_y) = e^{-q|z-D|} - \frac{e^{-q(|z|+D)}}{1+2\lambda q}$, and $W(k_x, k_y) = e^{-q|z-D|} sign(z - D) - \frac{e^{-q(|z|+D)}}{1+2\lambda q} sign(z)$. The in-plane components of the EMD magnetic fields have a jump at $z = 0$ which should be taken into account. The z-component of the dot's magnetic field is depicted in Fig.4. The magnetic field of the dot changes strongly across the dot's circumference due to large values of $\nabla \cdot \mathbf{M}$ there.

If vortices are present in the SC film then the total magnetic field is a linear superposition of the field from the EMD and that of the vortices. Recall that the z-component of the magnetic field due to a singly quantized SC vortex centered at the origin [24], [25], [26] reads

$$B_v^z(x, y, z) = \frac{\phi_0}{2\pi} \int_0^\infty \frac{q J_0(q\sqrt{x^2 + y^2}) e^{-q|z|}}{1 + 2\lambda q} dq \tag{2.44}$$

Assume that there are an N spontaneously created vortex in the superconductor. If $N > 1$ superconducting vortices the interaction of the vortices with the dot tries to lower the energy of the system due to its attractive nature while it is increased by the repulsive vortex-vortex interaction. If N vortices are coupled to the FM dot then I can recast the energy E of the EMD-SC system using the identity $\int d^2x \longrightarrow \frac{1}{4\pi^2} \int d^2k$. Then

$$E = N\epsilon_0 ln(\frac{\lambda}{\xi}) + \epsilon_0 \lambda \sum_{i=1}^{N} \sum_{j \neq i}^{N} \int_0^\infty \frac{J_0(\kappa|\rho_i - \rho_j|)}{1 + 2\lambda\kappa} d\kappa$$

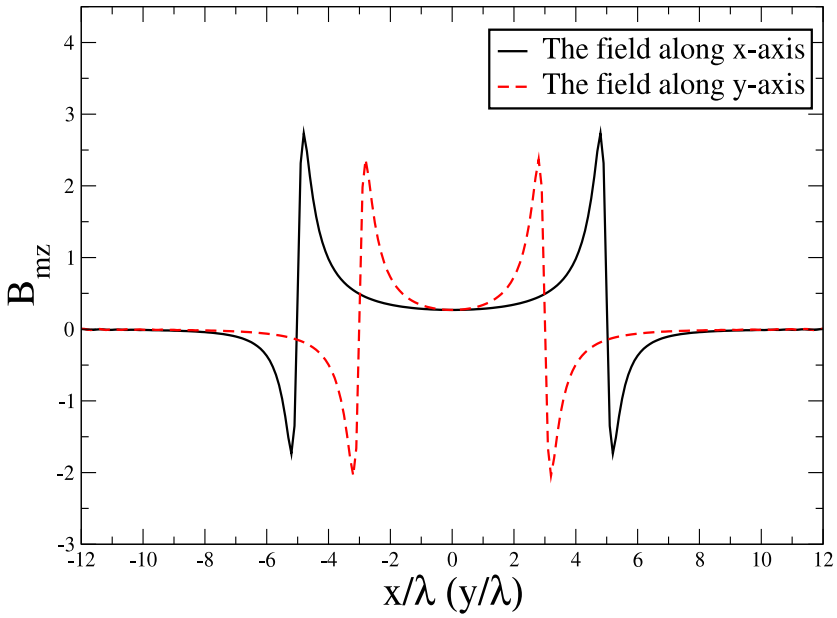

Fig. 4. The magnetic field in units of $\frac{2m_0}{\lambda}$ measured along the semi major axis (solid line) and semi-minor axis (dashed line) for EMD with $R_1 = 5$ and $R_2 = 3$

$$-\frac{m_0\phi_0 R_1 R_2}{\pi}\sum_{i=1}^{N}\Gamma(R_1, R_2, x_i, y_i) + E_{mm} \tag{2.45}$$

where κ has a dimension of inverse length and the function $\Gamma(R_1, R_2, x_i, y_i)$ is defined as

$$\Gamma(R_1, R_2, x_i, y_i) = \int \frac{J_1(G(k_x, k_y))e^{i(k_x x_i + k_y y_i)}}{G(k_x, k_y)\,(1 + 2\lambda q)} d^2q \tag{2.46}$$

Vortex configurations for $N = 1$ and $N = 2$ are shown in Fig. 5 and Fig. 6. For $N = 1$, the vortex appears under the center of the dot while for $N = 2$, vortices centers are located on the semi-major axis at equal distances from the center of the dot to minimize the total energy of the system. The degeneracy of the two vortex locations in the case of circular dot on the top of the SC film is lifted by the shape anisotropy of

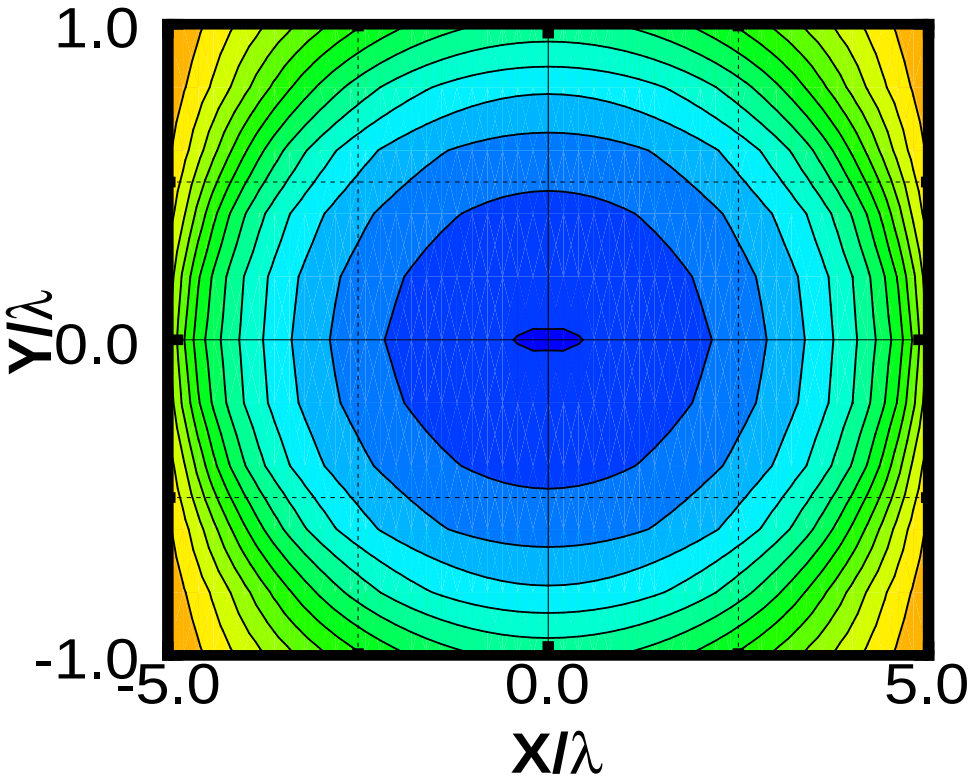

Fig. 5. Energy profiles for $N = 1$ in the EMD-SC system. The EMD has major (minor) axis $R_1 = 5\lambda (R_2 = \lambda)$ and $\delta_m = 3$.

the dot elliptic dot. The creation of vortex configurations with $N > 2$ requires larger values of δ_m to overcome the Pearl energy and the repulsive vortex-vortex interaction. Vortex arrangements of $N > 2$ depend on the ratio $\frac{R_2}{R_1}$. For $R_2 \sim \lambda$, vortices would line up forming a straight chain of vortices extending under the semi-major axis of the dot. When $R_2 \gg \lambda$, the arrangement of vortices becomes more complex. Energy and vortex lattice structure for $N \gg 1$ can be found numerically by minimizing the total energy of the system given by Eq.(2.45).

The energy of a single vortex depends on the eccentricity of the dot. To study this dependence, the energy of a single SC vortex coupled to an FM dot of fixed R_1

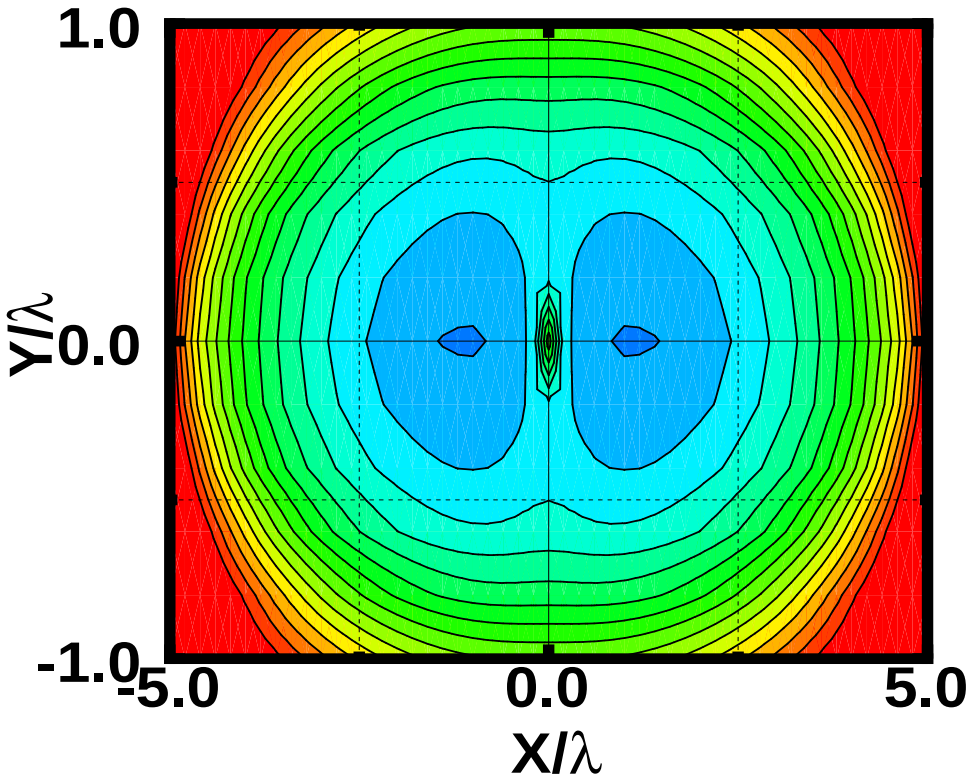

Fig. 6. Energy profile for $N = 2$ in the EMD-SC system. The EMD has major (minor) axis $R_1 = 5\lambda(R_2 = \lambda)$ and $\delta_m = 5$.

and variable R_2 must be calculated. The energy dependence on R_2 is represented by the solid curve in Fig.7. This shows that the lowest energy for $N = 1$ configuration is reached when $R_2 = R_1$. However, this does not imply that spontaneous creation of superconducting vortices is more energy favorable if the dot is circular. This is because the magnetic flux supplied by the dot is maximum when $R_1 = R_2$. To better understand this, I compare the energy necessary to spontaneously create a single vortex by an elliptic dot with fixed R_1 and varying R_2 to the energy of a vortex created by a circular dot with the same per unit area magnetization m_0 and radius $R_c = \sqrt{R_1 R_2}$. The magnetic flux due to both dots is equal since their areas are equal.

The curves in Fig.7 shows that the creation of vortices by an elliptic dots is more energy favorable than those created by circular ones and has the same magnetic flux. The difference between the two curves is reminiscent of the shape anisotropy of the FM dot.

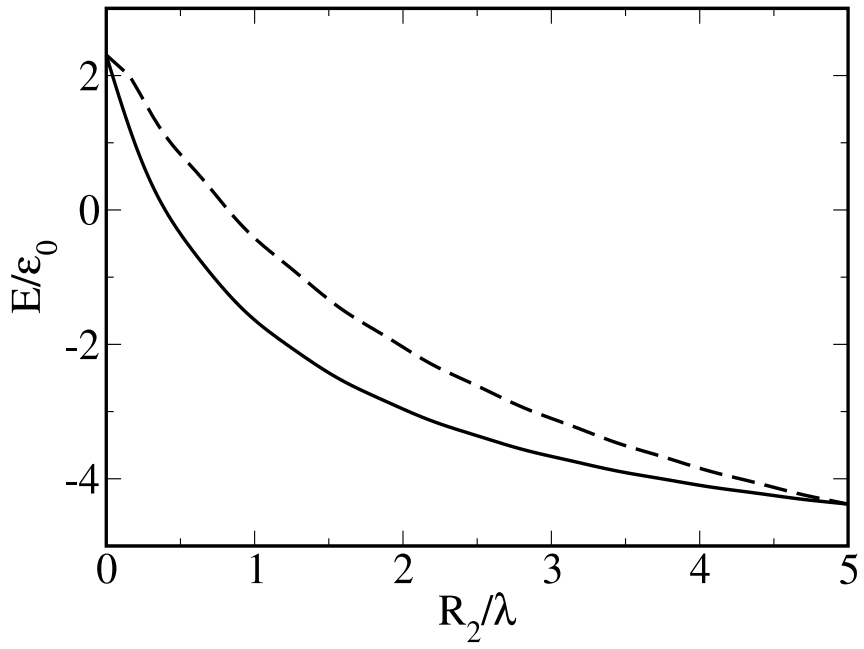

Fig. 7. The solid line is energy of a single vortex in the presence of an elliptic dot whose semi-major axis $R_1 = 5\lambda$ as a function of R_2. The dashed line is the energy of a single vortex created by a circular dot of radius $R_c = \sqrt{R_1 R_2}$. In both cases $\delta_m = 8$

The appearance of a vortex under the dot changes the energy of the system by an amount of $\Delta = U_{sv} + U_{vv} + U_{mv}$. A vortex appear when $\Delta = 0$. This criterion produces a surface in $3D$ space parametrized by $\frac{R_1}{\lambda}$, $\frac{R_2}{\lambda}$. The surface $\Delta = 0$ separates regimes with and without vortices. Phase transitions from $N = 0$ regime to $N = 1$ and $N = 2$ regimes are shown in Fig.8. Note that for strongly eccentric dot *i.e.*

$R_2 \ll R_1$ the spontaneous creation of vortices requires large values of δ_m due to the small stray field of the dot.

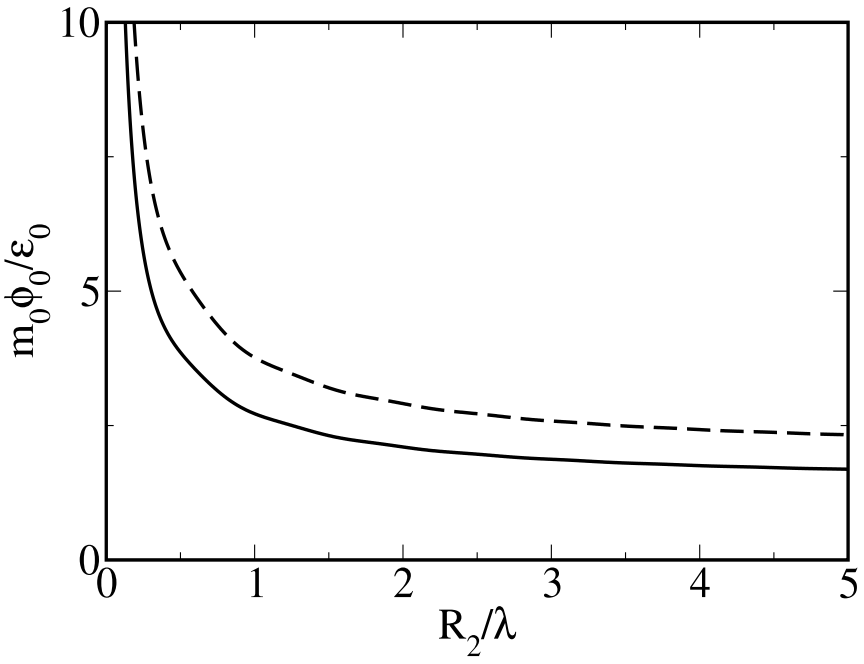

Fig. 8. The solid (dashed) curve separate the regime without vortices from the regimes with $N = 1$ ($N = 2$) vortices in the SC for $R_1 = 5\lambda$.

Now, consider a square array of identical elliptic FM dots on the top of a superconducting thin film. Let all dots have their semi-major axis aligned along the x-axis, and let them be well separated so that the dipolar interaction between them can be ignored. If δ_m is larger than a critical value then vortices appear under the dots. Due to the conservation of topological charge, an equal number of antivortices will appear in the regions between the dots. In the presence of the antivortices the total energy of the system must include their interaction with the dot array and vortices and other antivortices in the system. For a large enough array and a filling of one vortex per dot, vortices appear under the centers of the dots while antivortices will

appear at the centers of the unit cells. This is so only if finite size effects are ignored. These effects violate the symmetry of the vortex lattice, thus causing a shift in the locations of vortices and antivortices. Pinning forces acting on vortices are due to their interaction with the FM dots array and the vortex-antivortex interaction. Since the dots are well separated, the i-th vortex feels mostly the pinning potential created by the dot above it, given by (2.45) as

$$U_{mv} = -\frac{m_0\phi_0 R_1 R_2}{\pi}\Gamma(R_1, R_2, x_i, y_i) \tag{2.47}$$

The pinning by antivortices is isotropic and regular and can be represented by a two-dimensional washboard potential. The pinning force exerted by the FM dot on a single vortex in the SC is derivable from U_{mv} and its components are

$$F_j(x_i, y_i) = -\frac{\imath m_0\phi_0 R_1 R_2}{\pi}\Xi_j(R_1, R_2, x_i, y_i) \tag{2.48}$$

where $j = x, y$. Here the function $\Xi_j(R_1, R_2, x, y)$ is defined as

$$\Xi_j(R_1, R_2, x, y) = \int \frac{k_j J_1(G(k_x, k_y))e^{i(k_x x + k_y y)}}{G(k_x, k_y)\,(1 + 2\lambda q)} d^2q \tag{2.49}$$

The pinning force exerted by the dot on a vortex in the SC can be calculated numerically. The results are depicted in Fig.9.

The shape anisotropy of the dot manifests itself in the pinning potential U_{mv} and the pinning forces. Anisotropic pinning forces imply anisotropic transport properties such as anisotropic critical current. In other words the critical current J_c for this system may depend on the angle θ between the driving current and the semi-major axis of the dots. It also must depend on δ_m and the eccentricity of the dots, so I write $J_c(\theta)$. For fixed value of δ_m and $\frac{R_2}{R_1}$, the strength of the transport anisotropy can be measured through the ratio $K_1 = \frac{J_c(\theta=\frac{\pi}{2})}{J_c(\theta=0)}$. To detect the effect of the dot's shape anisotropy on the transport properties of the underlying superconductor, one

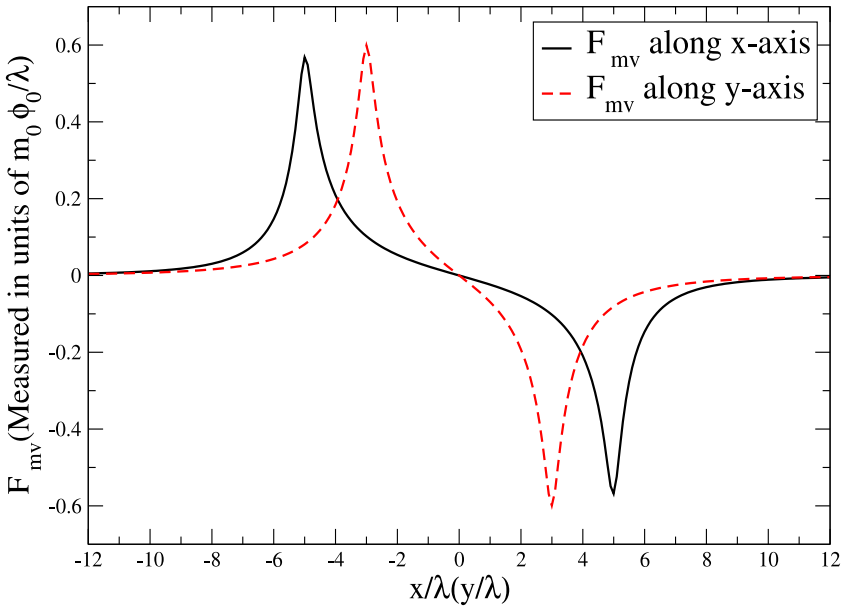

Fig. 9. The components of the pinning force exerted by the dot on a vortex in the SC for a dot of $R_1 = 5\lambda$ and $R_2 = 3\lambda$.

can perform resistivity measurements while changing θ. For an array of dots that are very eccentric, the measurements must reflect a decrease in the resistance of the sample as θ is increased down from 0 up to $\frac{\pi}{2}$. The full understanding of transport properties and the effect of the dot's shape anisotropy on vortex dynamics in this system has not yet been studied.

D. Vortex Manipulation by Cavities in a Magnetic Dot

Consider a superconducting thin film of thickness $d_s \ll \lambda$ in the xy-plane. Above it, a circular ferromagnetic dot of thickness $d_m \ll \lambda$ and radius R_1 whose magnetization points along the normal to the SC film is placed. Furthermore, assume that the dot contains a cavity of radius $R_2 < R_1$ is at the center of the dot. Such an annular

geometry can be realized as follows: (1) an FM dot of radius R_1 and thickness D_1 magnetized along the normal to the SC film is grown on the SC, and the dot is then covered by a thin layer of insulator oxide. (2) A second FM dot of radius $R_2 < R_1$ and thickness D_2 and opposite magnetization is grown on top of the insulating layer.

I assume that $D_1 + D_2 \sim \xi$ where ξ is the SC coherence length. Hence the thickness of the annulus can be ignored in the calculation because the field of the vortex does not change appreciably over a distance of the order of ξ. The FM and SC are separated by a thin layer of insulator oxide of thickness $D \ll \lambda$. The magnetization of the annulus can be written as

$$\mathbf{M}(\rho, z) = m_0 \Theta(R_2 - \rho)\Theta(\rho - R_1)\delta(z - D)\hat{z} \tag{2.50}$$

where m_0 is the magnetization per unit area. The overall system has an azimuthal symmetry, in Coulomb gauge ($\nabla \cdot \mathbf{A} = 0$) direct integration gives the magnetic vector potential

$$\mathbf{A}_m = 4\pi m_0 \lambda \hat{\varphi} \int_0^\infty q \frac{[R_2 J_1(qR_2) - R_1 J_1(qR_1)]\, J_1(q\rho)}{1 + 2\lambda q} e^{-q|z-D|} dq \tag{2.51}$$

The magnetic field produced by the annulus in the presence of the SC, by $\mathbf{B} = \nabla \cdot \mathbf{A}$, is

$$B_m^\rho = 4\pi m_0 \lambda \int_0^\infty \frac{q^2\, [R_2 J_1(qR_2) - R_1 J_1(qR_1)]\, J_1(q\rho)}{1 + 2\lambda q} e^{-q|z-D|} dq \tag{2.52}$$

$$B_m^z = 4\pi m_0 \lambda \int_0^\infty \frac{q^2\, [R_2 J_1(qR_2) - R_1 J_1(qR_1)]\, J_0(q\rho)}{1 + 2\lambda q} e^{-q|z-D|} dq \tag{2.53}$$

The total z-component of the magnetic field on the film is the sum of those from the magnetic annulus and from the vortex. The z-component of the magnetic field from the vortex behaves like $\frac{1}{\rho^2}$ at distances smaller than λ, and like $\frac{1}{\rho^3}$ at large

distances. The behavior of the z-component of the annulus magnetic field is shown in Fig.10. Let us assume that a vortex in the SC is located at point ρ_0 interacting

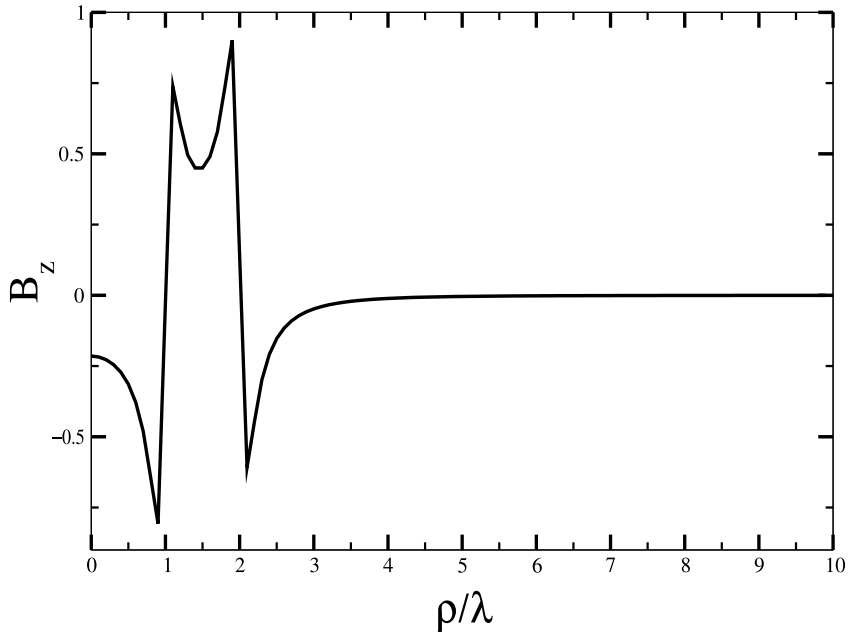

Fig. 10. The z-component of the annulus magnetic field on the surface of the superconductor. The annulus has a radii ($R_1 = \lambda, R_2 = 2\lambda$) and the field is measured in units of $\frac{4\pi m_0}{\lambda}$.

with the annulus then the total energy of the system is

$$\begin{aligned} E &= N\epsilon_0 ln(\frac{\lambda}{\xi}) - \epsilon_0\lambda\sum_{i=1}^{N}\sum_{j\neq i}^{N}\int_0^\infty \frac{J_0(q|\rho_i-\rho_j|)}{1+2\lambda q}dq \\ &\quad -\epsilon_m\sum_{i=1}^{N}\int_0^\infty \frac{(R_2J_1(qR_2)-R_1J_1(qR_1))\,J_0(q\rho_0)}{1+2\lambda q}dq \end{aligned} \tag{2.54}$$

If $\delta_m > 1$ then spontaneous creation of vortices is energy favorable. I numerically integrate (2.54) for $N = 1$ and plot the energy as a function of ρ_0. Clearly, the energy has a minimum in the region under the annulus i.e. $R_1 < \rho_0 < R_2$ as shown in Fig.11.

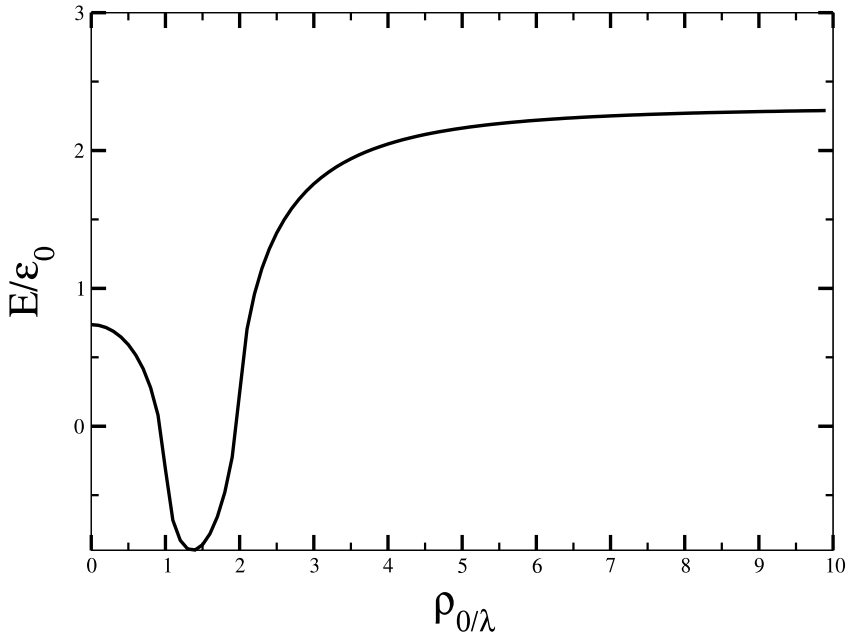

Fig. 11. The energy in units of ϵ_0 as a function of $\frac{\rho_0}{\lambda}$ for the case when $n = 1, \frac{\lambda}{\xi} = 10, R_1 = \lambda, R_2 = 2\lambda$ and $\delta_m = 10$.

The azimuthal symmetry of the annulus leads to a continuous set of equivalent locations for the vortex center along a circle of radius ρ_0. The interaction between the vortices and the magnetization is attractive and strongest in the region under the annulus while the vortex-vortex interaction is repulsive and decays logarithmically with the distance between two vortices if the distance between the two vortices is larger than λ. Therefore, if there are $N \leq [2\pi\frac{\rho_0}{\lambda}]$ singly quantized vortices in the superconductor then they will be uniformly distributed along the circumference of a circle whose radius is ρ_0. Otherwise, their exact distribution in the superconductor must be determined by numerically minimizing the total energy of the system.

The degeneracy found for the location of the vortex center is a direct result of the azimuthal symmetry of the annulus. Such a degeneracy can be eliminated by either

moving the cavity from the center of the dot or introducing new cavities into the dot. another opportunity is to use a non-circular annulus. Such modifications make the ground state manifold discrete instead of continuous as shown in the circular annulus case. Motivated by our work, Milosevic and Peeters [19] studied the dependence of the dependence of the energy of the system on the location of the cavity in the dot. It is found that when two identical cavities are brought together to form a figure eight shaped cavity at the center of the dot, the system has exactly two equivalent ground states. The probabilities are equal that the vortex is in either of these states. Such a feature makes this system useful for quantum computing.

E. Interaction Between a Superconducting Vortex and a Ferromagnetic Rod

Previous studies focused on cases in which the dimensionality D of the FM was either zero or two [1]-[22]. This corresponds to the action of a point dipole of a dot. To date no study has considered the interaction of vortices in a superconducting thin film with a ferromagnetic rod. The system I will study here consists of an SC thin film which contains a hole of radius R_1 pierced by a ferromagnetic columnar defect of radius R_2 and length $L > 0$, subject to the condition $R_1 - R_2 \sim \xi \ll \lambda$. The rod is uniformly magnetized in the direction perpendicular to the SC film, as shown in Fig.12. In this work, I will ignore the difference between the radius of the rod and that of the hole and put $R_1 = R_2 = R < \lambda$.

The magnetization of the rod can be expressed as

$$\mathbf{M}(\rho, \varphi, z) = M\Theta(R - \rho)\Theta(\frac{L}{2} - |z|)\mathbf{z} \tag{2.55}$$

The magnetic field produced by the FM penetrates the superconductor modifying

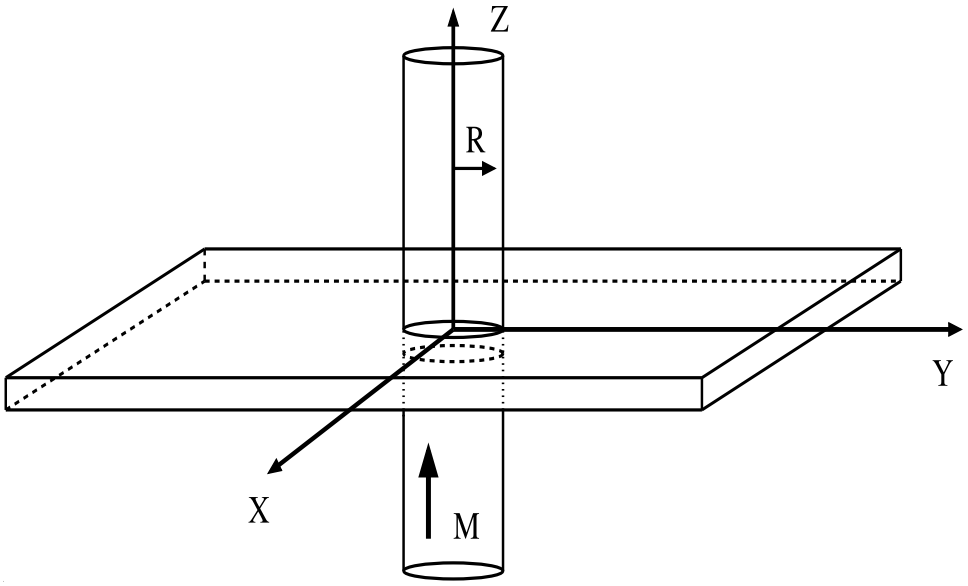

Fig. 12. A superconducting thin film pierced by a ferromagnetic nano rod of radius R, length L and magnetization M.

its screening current distribution. Within the London approximation the FM-SC system is described by the London-Maxwell equation. When Coulomb gauge ($\nabla \cdot \mathbf{A} = 0$) is employed the Fourier representation of the vector potential A_k^m due to the FM can be written as

$$\mathbf{A}_k^m = \frac{16\pi^2 \imath M R J_1(qR)}{k_z^2 + q^2} \left[\frac{2\sinh(\frac{qL}{4}) e^{-\frac{qL}{4}}}{q(1+2\lambda q)} - \frac{\sin(\frac{k_z L}{2})}{k_z} \right] \hat{\varphi}_q \tag{2.56}$$

The magnetic field produced by the magnetic nano-rod in the presence of the SC film can be calculated using $\mathbf{B}^m = \nabla \times \mathbf{A}^m$. The components of the rod's magnetic field are

$$B_z^m = 8\pi M R \int_0^\infty J_1(qR) J_0(q\rho) \left[\frac{\pi}{2\lambda^2 q^2} W(q,z,L) - \frac{\sinh(\frac{qL}{4}) e^{-q(|z|+\frac{L}{4})}}{1+2\lambda q} \right] dq \tag{2.57}$$

$$B_\rho^m = 8\pi MR\int_0^\infty J_1(qR)J_1(q\rho)\left[\frac{\pi}{2\lambda^2q^2}W(q,z,L) - \frac{\sinh(\frac{qL}{4})e^{-q(|z|+\frac{L}{4})}}{1+2\lambda q}\right]dq \quad (2.58)$$

where

$$\begin{aligned} W(q,z,L) &= sign(L-2z)\left[1-\cosh(\frac{q(L-2z)}{2}) + sign(L-2z)\sinh(\frac{q(L-2z)}{2})\right] \\ &+ sign(L+2z)\left[1-\cosh(\frac{q(L+2z)}{2}) + \sinh(\frac{q|L+2z|}{2})\right] \end{aligned} \quad (2.59)$$

However, I am interested in the value of the field in the plane of the superconductor, the z component of the field reduces at the SC film to

$$B_z^m(\rho) = 8\pi MR\int_0^\infty \frac{qJ_1(qR)J_0(q\rho)}{1+2\lambda q}(1-e^{-\frac{qL}{2}})dq \quad (2.60)$$

In the presence of a superconducting vortex, the total magnetic field at the surface of the film is the sum of the field of the FM rod and the field of the vortex itself. The z-component of the vortex magnetic field at the SC film surface is [24], [25], [26]

$$B_z^v(\rho) = \frac{\phi_0}{2\pi\lambda^2}\left[\frac{\lambda}{2\rho} - \frac{\pi}{8}\left(H_0(\frac{\rho}{2\lambda}) - N_0(\frac{\rho}{2\lambda})\right)\right] \quad (2.61)$$

where $H_0(x)$ and $N_0(x)$ are the zero order Struve and Neumann functions respectively [27]. The interaction between a superconducting vortex and a non-magnetic columnar defect was first considered by Mkrtchyan and Schmidt [23], and later by Buzdin *et.al.* [28], [29], [30], [31], [32]. In these studies, it was shown that the pinning potential U_p created by a non magnetic columnar defect of radius $R > \sqrt{2}\xi$ is

$$U_p(\rho) = \begin{cases} -\epsilon_0\ln(\frac{R}{\sqrt{2}\xi}), & \rho < R \\ \epsilon_0\ln\left[1-\left(\frac{\sqrt{2}R}{\sqrt{2}\rho+\xi}\right)^2\right], & R < \rho < \lambda \end{cases}$$

If the columnar defect is ferromagnetic then an extra contribution to the pinning would appear due to the magnetic interaction between the superconductor and ferromagnet. In the presence of N singly quantized vortices in the superconductor,

the total energy of the system is made up of five different contributions and can be written as

$$U = U_{sv} + U_{vv} + U_p + U_{mv} + U_{mm} \tag{2.62}$$

where U_{sv} is the energy of N non-interacting singly quantized vortices, U_{vv} is the vortex-vortex interaction, U_p is the pinning potential due to the hole without the magnetic rod, U_{mv} is the interaction energy between the FM and SC, and U_{mm} is the FM dot self interaction. In [16], it was shown that the total energy of the system can be written as:

$$U = \int \left[\frac{n_s \hbar^2}{8m_e} (\nabla\varphi)^2 - \frac{n_s \hbar e}{4m_e c} (\nabla\varphi \cdot \mathbf{A}) - \frac{1}{2}\mathbf{M}\cdot\mathbf{B} \right] d^3x \tag{2.63}$$

where n_s is the three-dimensional superconducting electrons density and m_e is their effective mass. $\hbar$ and c are the Planck constant and the speed of light respectively. The vectorial quantities $\mathbf{A}$, and $\mathbf{B}$ are the total vector potential and magnetic field due to the N SC-vortices and the ferromagnetic rod. The phase gradient of the SC order parameter in the presence of N vortices is $\nabla\varphi = \sum_{n=1}^{N} \frac{(\rho-\rho_n)\times\hat{z}}{|\rho-\rho_n|^2}$, where $\rho_{\mathbf{n}}$ is the location of the n-th vortex.

Unlike previous cases, here the energy in (2.63) is a sum of $3D$ integrals; however, some of these integrals can be made $2D$ while the others must be performed in three dimensions. In the presence of $N > 1$ superconducting vortices, the interaction of the vortices with the rod tries to lower the energy of the system due to its attractive nature whereas the energy is increased by the repulsive vortex-vortex interaction. The total energy for a system of a superconducting vortex and a ferromagnetic columnar defect is

$$U_1(\rho) = \epsilon_0 \ln(\frac{\lambda}{\xi}) + U_p(\rho_0) + U_{mm} - 2\epsilon_m \frac{R}{\lambda} \int_0^\infty \frac{J_0(q\rho_0)J_1(qR)(1-e^{-\frac{qL}{2}})}{q(1+2\lambda q)} dq \tag{2.64}$$

Here I employ the energy scale for the interaction between the FM and SC

$$\tilde{\epsilon}_m = M\phi_0\lambda \tag{2.65}$$

Note that $\tilde{\epsilon}_m$ is now defined in terms of the $3D$ magnetization. The term U_{mm} is the self interaction of the FM rod. To simplify the calculations, I will limit the discussion to the case when $L \to \infty$. Numerical calculations show that the total energy U_1 has a minimum at $\rho_0 = 0$, so the vortex center must be on the axis of the rod.

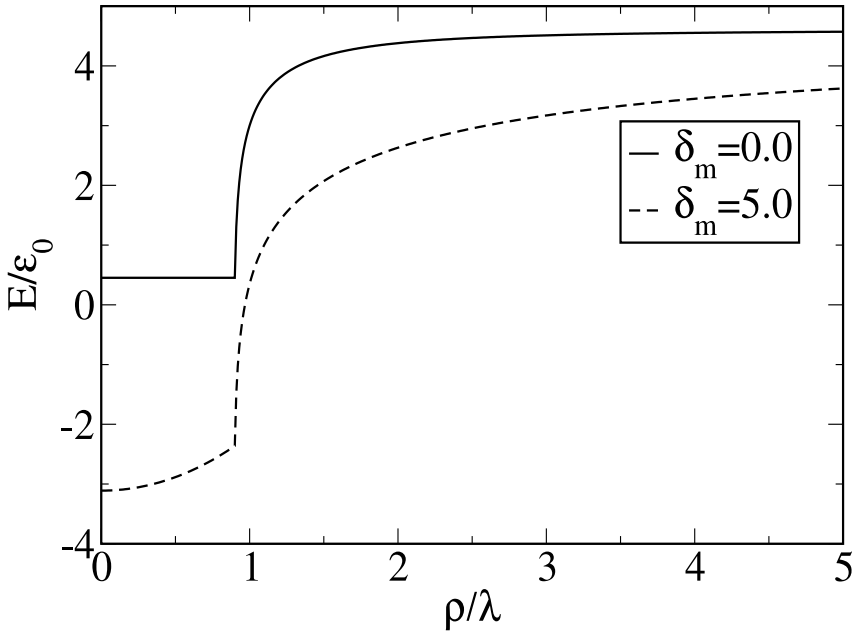

Fig. 13. The total energy of the CD-SV system for $\lambda = 1000$nm, $\xi = 10$nm and the radius $R = 900$nm.. The solid line is for the case when the CD is non-magnetic while the dashed one is for ferromagnetic CD.

The various terms in Eq.(2.64) shows that if the magnetization of the rod exceeds

a threshold value then the spontaneous creation of vortices becomes energy favorable. The energy profile for a single vortex coupled to a columnar defect is shown in Fig.13. The solid line represents the energy of the system for a non-magnetic defect and the dashed line is for a ferromagnetic defect. Note that for a non-magnetic cavity, the model of Mkrtchyan and Schmidt [23] leads to zero pinning force if $\rho_0 < R$, whereas in the present case the pinning potential is stronger and the pinning force does not vanish if $\rho_0 < R$. The pinning force exerted by the FM rod on a vortex in the SC film at ρ_0 is oriented along the radial direction and is given by

$$F_\rho(\rho) = -\frac{\partial U_p(\rho)}{\partial \rho} - 2\tilde{\epsilon}_m \frac{R}{\lambda} \int_0^\infty \frac{J_1(q\rho_0) J_1(qR)(1 - e^{-\frac{qL}{2}})}{(1 + 2\lambda q)} dq \tag{2.66}$$

The spontaneous creation of a vortex in the SC changes the energy of the system by $\Delta = U - U_{mm}$. Therefore, if I set $\Delta = 0$ then I can find the threshold value of the magnetization Fig.14 at which spontaneous vortex creation becomes energy favorable. Taking $R = 500$ nm and $\lambda = 1000$ nm, I find that the threshold value of magnetization is approximately $M = 388$ G. Configurations with a larger number of vortices are found by minimizing the total energy of the system with respect to the positions of vortices and antivortices. However, one should be cautious here because the net flux through the SC film is not zero except when $L \to \infty$, unlike the case when the FM is two dimensional structure placed outside the SC. In the present case the FM penetrates the SC despite the fact that the FM and SC are electronically separated by a thin ring of radius $R_1 - R_2$; therefore, the flux neutrality principle that was used for problems with $2D$ FM textures must be modified in cases like the present case.

In this section, I studied the interaction between SC vortices and an FM rod penetrating the plane of the SC. To study such interaction I extended the theory of vortex interaction with non magnetic cavities to include the case when the cavity

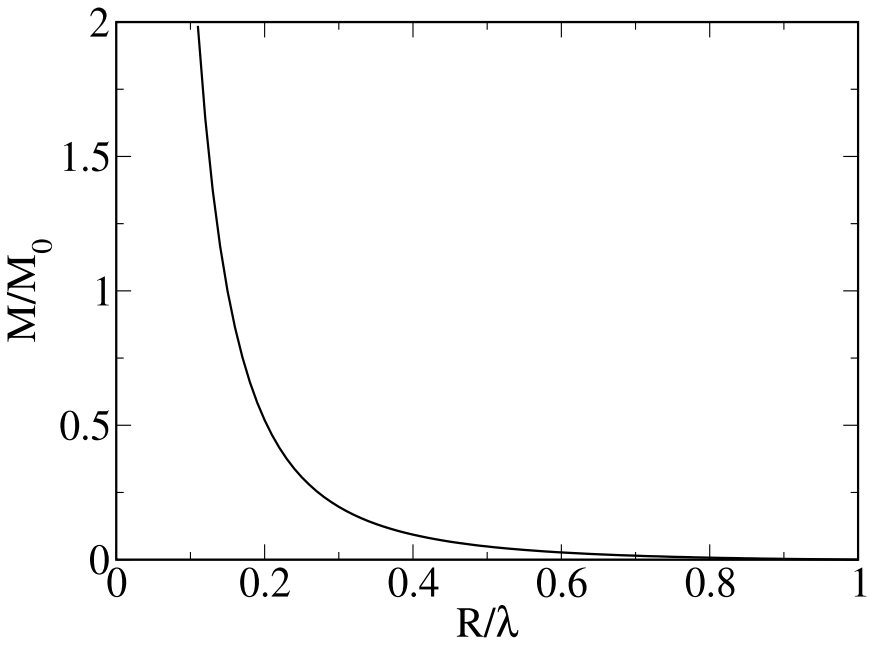

Fig. 14. The curve represents the threshold value of the magnetization of the rod in units of $M_0 = \phi_0/\pi\lambda^2$.

is filled with ferromagnetic material. I calculated the pinning potential and force supplied by the FM rod. I showed that if the FM rod magnetization exceeds a critical value then vortices spontaneously appear in the ground state of the system. The phase transition from vortexless phase to phase with one vortex is studied and the threshold value of the magnetization is found as a function of the radius of the rod.

CHAPTER III

TRANSPORT IN FERROMAGNETIC-SUPERCONDUCTING BILAYERS

Recently, Erdin *et.al.*[20] studied the equilibrium structure of a FM-SC bilayer (FSB). They have proved that it represents a two-dimensional periodic stripe domain structure consisting of two equivalent sub-lattices, in which both the magnetization $m_z(\mathbf{r})$ and the vortex density $n_v(\mathbf{r})$ alternate. Thus, they predicted spontaneous violation of the translational and rotational symmetry in the bilayer. In this chapter I study the transport properties of the FSB. They are associated with the driving force acting on the vortex lattice due to an external electric current. I show that the FSB exhibits strong anisotropy of the transport properties: the bilayer may be superconducting for the current parallel to the domain walls, and resistive when the current is perpendicular to them.

The force acting on a vortex from other vortices, which determines the value of critical current, can be characterized as the periodic pinning. An extensive development of theory and experiment related to the pinning and its influence on transport in superconductors was discussed in an exhaustive review by Blatter *et al.* [2]. This work differs from the studies considered in this review by two features. First, in the preceding works the magnetic field was assumed to be constant in space, whereas in the present problem the average magnetic field is zero, but is strongly inhomogeneous in space. Therefore, in the present system equal numbers of vortices and antivortices participate in the motion. Second, in these works the pinning force was assumed to be random, whereas in this work the dominant pinning forces are periodic and regular. Martinoli *et al.* [5] created artificially periodic pinning barriers in superconducting films by modulating their thickness periodically. The main difference between their modulated structure and the one considered in in this work is that the domains in the

FSB are not confined to the crystal lattice and can move together with the vortices.

Periodic pinning forces in the direction parallel to the stripes do not appear in continuously distributed vortices, their reappearance is associated with the discreteness of the vortex lattice. Therefore, I need to modify the theory [20] to incorporate the discreteness effects. Assume that the saturation magnetization per unit area of the FM film is m and its width is L. The energy necessary to create a single Pearl vortex [24] in the superconductor is $\epsilon_{v0} = \epsilon_0 \ln(\frac{\lambda}{\xi})$, It was shown in [20] that the interaction between the superconducting vortices and the magnetization in the stripe structure renormalizes the single-vortex energy to the value $\tilde{\epsilon_v} = \epsilon_{v0} - m\phi_0$ which must be negative to allow development of the stripes. The density of the superconducting vortices increases when approaching the domain walls and in the continuous approximation [20] it can be expressed as

$$n_v(x) = \frac{\pi\tilde{m}}{L\phi_0} \frac{1}{\sin(\frac{\pi x}{L})} \tag{3.1}$$

where $\tilde{m} = m - \frac{\epsilon_{v0}}{\phi_0}$ is the renormalized magnetization of the FM stripe. and L is the stripe domain width. The vortices spontaneously appear in the superconductor. I assume that the vortices inside one stripe are arranged in parallel chains as in Fig. 15. Each chain is periodic with the same lattice constant b along the chain, whereas the distance a_k between the k-th and the $(k+1)$-th chain depends on k. The correspondence between this discrete arrangement and the continuous approximation [20] is established by the requirement that the local vortex density $n_v(x_k)$ calculated in [20] must equal $(ba_k)^{-1}$. The coordinate x_k is determined in terms of a_k as a sum: $x_k = \sum_{k'=0}^{k-1} a_{k'}$. For definiteness I choose the origin at the center of the stripe. I assume that the total number of the vortex chains $2N$ in a stripe is large. Then some of them are located very close to the domain walls. Considering the vortex chain nearest to the domain wall (with the index, N), I put $n_v(x_N) = \frac{1}{ba_N}$. On the other

hand, $x_N = L - a_N$. Since $\frac{a_N}{L} \ll 1$, I find, $b = \frac{\phi_0}{\tilde{m}}$. The total number of chains in a stripe is $2N$, where

$$N = b\int_0^{L-\lambda} n_v(x)dx = \frac{1}{2}\ln(\frac{L}{\lambda}) \tag{3.2}$$

I must cut off the integration (and summation) at a distance $\sim \lambda$ from the domain wall, where the continuum approximation breaks. Thus the minimum value of a is λ.

When transport current passes through the superconducting film, the vortices start to move. To simplify the problem I assume that all vortices in each stripe move together as well as all antivortices in the neighboring stripe do.

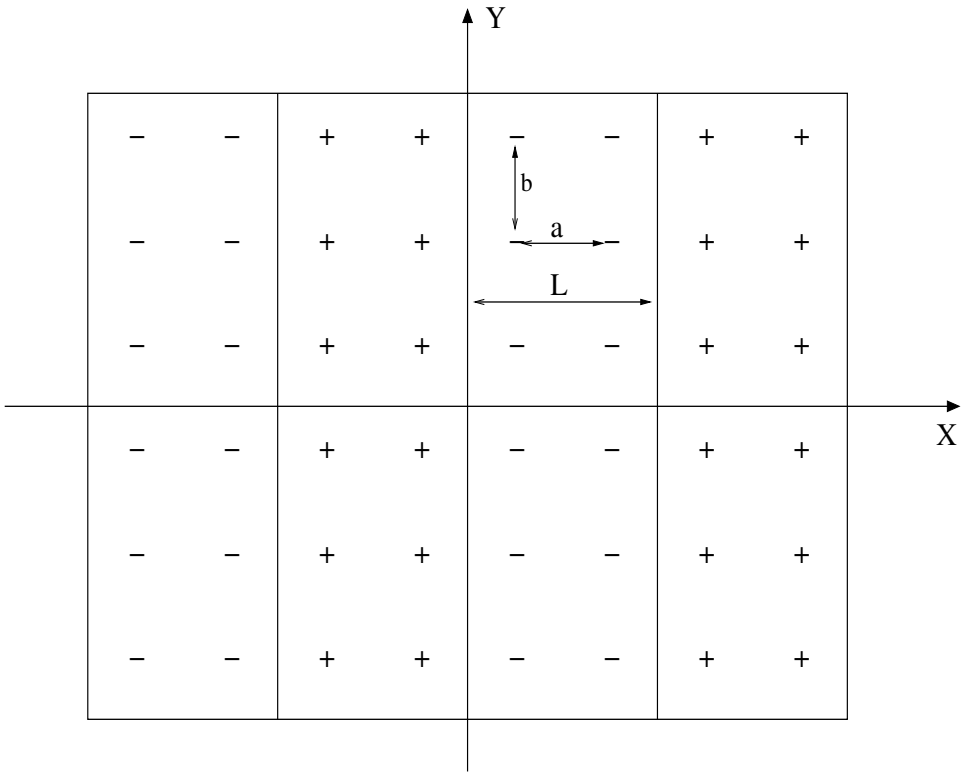

Fig. 15. Schematic vortex distribution in the FM-SC bilayer. The sign ± refers to the vorticity of the trapped flux.

I denote vortex and antivortex positions by $\mathbf{r}_+ = (x_+, y_+)$ and $\mathbf{r}_- = (x_-, y_-)$, respectively. The forces acting on a moving vortex are the Magnus force $\mathbf{f}_m$, the

friction force $\mathbf{f}_f$, and the periodic pinning force $\mathbf{f}_p$.The Magnus force is

$$\mathbf{f}_m = \pi n_s \hbar d_s (\mathbf{v_s} - \dot{\mathbf{r}}) \times \hat{\mathbf{z}} \tag{3.3}$$

where n_s is the superconducting electron density, v_s is the velocity of the superconducting electron and $\dot{\mathbf{r}}$ is the vortex velocity. The viscous (friction) force is $\mathbf{f}_f = -\eta\dot{\mathbf{r}}$ where $\eta = \frac{\phi_0 H_{c2} d_s}{\rho_n c^2}$ is the Bardeen-Stephen drag coefficient [33], with H_{c2} the upper critical magnetic field, ρ_n the resistivity of the superconducting sample in the normal state, and c is the speed of light.

The periodic pinning forces are due to the interaction of the vortex with the pinning centers and the domain walls. In the FM-SC bilayer the pinning force is due to the interaction of the domain walls with the vortices and antivortices and the vortex-vortex interaction U_{vv} given by:

$$U_{vv} = \frac{1}{2} \int \int n_v(\mathbf{r}) V(\mathbf{r} - \mathbf{r}') n_v(\mathbf{r}') d^2\mathbf{r} d^2\mathbf{r}' \tag{3.4}$$

where $V(\mathbf{r} - \mathbf{r}')$ is the pair interaction between a vortex located at $\mathbf{r}$ and another at $\mathbf{r}'$. When $|\mathbf{r} - \mathbf{r}'| \gg \lambda$ the pair interaction can be written as

$$V(\mathbf{r} - \mathbf{r}') = \frac{\phi_0^2}{4\pi^2} \frac{1}{|\mathbf{r} - \mathbf{r}'|} \tag{3.5}$$

The interaction energy between two parallel chains located at x_l and $x_{l'}$ and vertically shifted with respect to each other by an interval bs ($s \ll 0$), is

$$U(x_l, x_{l'}, s) = \sum_{n,m=1}^{N_0} \frac{\frac{\phi_0^2}{8\pi^2}}{\sqrt{(x_l - x_{l'})^2 + (n - m - s)^2 b^2}} \tag{3.6}$$

where N_0 is the number of vortices or antivortices in a single chain. For infinite chains

($N_0 \to \infty$) Eq.(3.6) can be rewritten as

$$U(x_l, x_{l'}, s) = \sum_{k=-\infty}^{\infty} \frac{\frac{N_0\phi_0^2}{8\pi^2}}{\sqrt{(x_l - x_{l'})^2 + (k-s)^2 b^2}} \tag{3.7}$$

The sum in (3.7) can be calculated using the Poisson summation formula [27]. Since the force is zero in the continuum approximation, it is possible to retain the lowest non-zero harmonic in the Poisson summation. Thus, I arrive at the following interaction energy of two chains:

$$U(x_l, x_{l'}, s) = \frac{N_0\phi_0^2}{4\pi^2 b}\cos(2\pi s)\chi_{ll'} \tag{3.8}$$

where $\chi_{ll'} = e^{-2\pi\frac{|x_l - x_{l'}|}{b}}$. The distance between two chains $|x_l - x_{l'}|$ exceeds or equals λ, so $\chi_{ll'} \sim \chi = e^{-\frac{2\pi\lambda}{b}}$. A typical value of $\chi_{ll'}$ is $e^{-\frac{\delta_m}{4\pi}}$, so χ is very small near the superconducting transition temperature and for thicker FM films.

I conclude that the amplitude of the periodic potential for displacements parallel to the domains, in units of the vortex self energy scale ϵ_0, is exponentially small near the transition temperature. Relative displacements in perpendicular direction have energy barrier $\sim \epsilon_0$ even in the continuum approximation. I model the restoring pinning forces by simple sine dependencies

$$f_x^p = -f_\perp \sin(\frac{2\pi}{a}(x_+ - x_-)) \tag{3.9}$$

$$f_y^p = -f_{||} \sin(\frac{2\pi}{b}(y_+ - y_-)) \tag{3.10}$$

where $f_\perp \sim \frac{\epsilon_0}{a}$ and $f_{||} \sim \frac{\epsilon_0}{b}e^{-\frac{\delta_m}{4\pi}} \ll f_\perp$.

The equations of motion for the vortex and antivortex are derived from the momentum conservation principle such that

$$f_f + f_m + f_p = 0 \tag{3.11}$$

If the supercurrent is perpendicular to domains, the equations of motion for a vortex and antivortex are:

$$\eta \dot{y}_+ = F - \frac{F}{v_s}\dot{x}_+ - f_{||}\sin(\frac{2\pi}{b}(y_+ - y_-)) \tag{3.12}$$

$$\eta \dot{x}_+ = \frac{F}{v_s}\dot{y}_+ + f_{\perp}\sin(\frac{2\pi}{a}(x_+ - x_-)) \tag{3.13}$$

$$\eta \dot{y}_- = -F + \frac{F}{v_s}\dot{x}_- + f_{||}\sin(\frac{2\pi}{b}(y_+ - y_-)) \tag{3.14}$$

$$\eta \dot{x}_- = -\frac{F}{v_s}\dot{y}_- - f_{\perp}\sin(\frac{2\pi}{a}(x_+ - x_-)) \tag{3.15}$$

where $F = \pi n_s \hbar d_s v_s$. If the current is smaller than a critical value J_c, then Eq.(3.12-3.15) has a static solution

$$x_+ = x_- = \frac{Fb}{4\pi\eta v_s}\arcsin(\frac{F}{f_{||}}) \tag{3.16}$$

$$y_+ = -y_- = \frac{b}{4\pi}\arcsin(\frac{F}{f_{||}}) \tag{3.17}$$

This is valid for $F \leq f_{||}$, and satisfies the condition that $x_\pm = y_\pm = 0$ when $F = 0$. For $F > f_{||}$ or, equivalently, if the current is larger than its critical value, the vortices and antivortices begin to move. The solution of Eq.(3.12-3.15) for $F > F_{||}$ reads:

$$x_+ - x_- \;\; = \;\; 0 \tag{3.18}$$

$$x_+ + x_- = \frac{F}{\eta v_s}(y_+ - y_-) \tag{3.19}$$

$$y_+ - y_- = \frac{b}{\pi}\arctan(\frac{f_{||}}{F} + \sqrt{1 - \frac{f_{||}^2}{F^2}}\tan(\omega_0^{\perp} t)) \tag{3.20}$$

$$y_+ + y_- = 0 \tag{3.21}$$

where

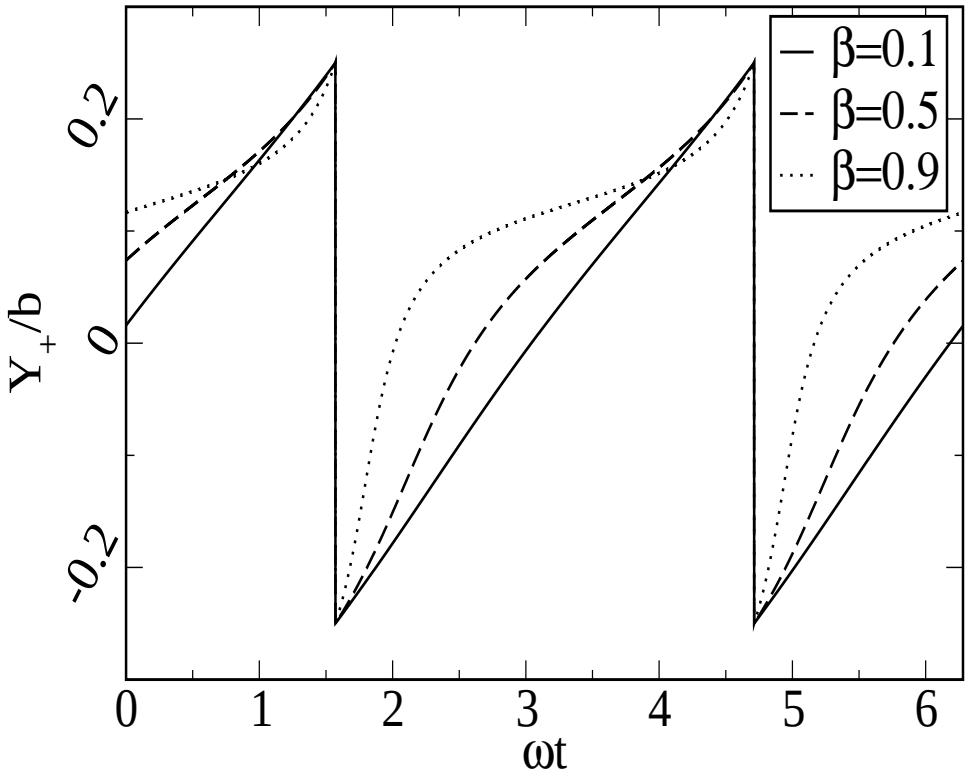

Fig. 16. The vortex displacement as a function of time in the overcritical regime. Time is measured in units of $\frac{1}{\omega_0^{\perp}}$ and y_+ in units of b and $\chi = 10^{-4}$.

$$\omega_0^{\perp} = \frac{2\pi\eta v_s^2\sqrt{b^2F^2 - \chi^2\epsilon_0^2}}{b^2(F^2 + \eta^2 v_s^2)} \tag{3.22}$$

is the Josephson frequency. Thus the vortices and antivortices acquire the same velocity components $v_{+x} = v_{-x}$ in the direction of the current and opposite velocity components $v_{+y} = -v_{-y}$ in the direction perpendicular to the current. The domain

walls do not interfere with such a motion if they move in the direction of the current with the same velocity $v_{dw} = v_{+x} = v_{-x}$ as vortices and antivortices. Such a motion is a Goldstone mode. The solution (3.18-3.21) displays an oscillatory motion of the vortices and antivortices in the direction parallel to the domain walls, in addition to their motion together with the domain walls along the direction of the current. Higher harmonics of the vortex motion can be calculated analytically. The distribution of vortices (antivortices) is inhomogeneous in the direction perpendicular to the domains. The local electric field $\mathbf{E}$ due to the vortex motion is related to its time-average velocity $< \mathbf{v}_+ >$ [2] via

$$\mathbf{E} = -\frac{q_v \phi_0}{c} n_v(\mathbf{r})(< \mathbf{v}_+ > \times \hat{\mathbf{z}}) \tag{3.23}$$

Therefore, the local field produced by vortices in the direction parallel to the domains is equal but opposite in sign to the one produced by antivortices, while the local field produced by vortices and antivortices in the direction perpendicular to the domains has both equal magnitude and sign. The time-average components of the vortex (antivortex) velocity over a period $T = \frac{2\pi}{\omega_0^{\perp}}$ are

$$< \mathbf{v}_{+y} > = \pm \frac{\eta \sqrt{F^2 - f_{||}^2}}{(\eta^2 + \frac{F^2}{v_s^2})} \tag{3.24}$$

$$< \mathbf{v}_{+x} > = \frac{F < v_{+y} >}{\eta v_s} \tag{3.25}$$

The time-averaged local field components are

$$E_x = -\frac{\eta \tilde{m}}{ac} \frac{\sqrt{F^2 - f_{||}^2}}{(\frac{F^2}{v_s^2} + \eta^2)} \tag{3.26}$$

$$E_y = \mp \frac{\tilde{m} F}{a v_s c} \frac{\sqrt{F^2 - f_{||}^2}}{(\frac{F^2}{v_s^2} + \eta^2)} \tag{3.27}$$

The upper signs in Eq.(3.24) and Eq.(3.27) refer to the vortex velocity and field for vortices along the domain while the lower sign refers to those for antivortices. A non-zero average electric field due to all vortices and antivortices in the FSB appears only in the direction perpendicular to the domains. The applied current **J** and Magnus force **F** are related by

$$\mathbf{F} = \frac{\phi_0 d_s}{c}\mathbf{J} \times \hat{z} \tag{3.28}$$

The perpendicular critical current $J_c^{\perp}$ can be found by equating the Magnus force F_c and the pinning force which gives $F = \frac{\epsilon_0 m \chi}{\phi_0}$. Taking $\chi = 10^{-4} - 10^{-2}$, $b = 10^{-4} - 10^{-5}$ cm, and $n_s = 10^{22}$ cm^{-3} yields $J_c^{\perp} \sim 10^3 - 10^5$ A/cm^2. When the current flows parallel to the stripes, the FM domain walls stay at rest while vortices and antivortices move both parallel and perpendicular to the domains. The equations of motion in this case are similar to their counterparts in the previous case with the exception that the domain walls do not move. The solution of equations of motion for vortices and antivortices shows that they move opposite to one another both in the x and y directions. Their motion along x is oscillatory with fundamental frequency

$$\omega_0^{||} = \frac{2\pi\eta v_s^2\sqrt{a^2F^2 - \epsilon_0^2}}{a^2(F^2 + \eta^2 v_s^2)} \tag{3.29}$$

The motion of vortices and antivortices in the parallel direction proceeds until the distance between them becomes the half-lattice spacing $\frac{b}{2}$. Once the vertical shift between the vortices and antivortices reaches $\frac{b}{2}$, their motion freezes. The parallel critical current in this case is $J_c^{||} = \frac{n_s \mu_B}{2a}$, the lattice spacing a is of the order of $\lambda \sim 10^{-5} - 10^{-4}$ cm, hence the critical current $J_c^{||}$ is of the order $10^7 - 10^8$ A/cm^2, which is at least 10^2 times larger than the critical current for parallel current. Therefore, the system may be superconducting for current parallel to the stripes, but exhibit

finite resistance for perpendicular current.

The difference in the critical currents for parallel and perpendicular directions is due to the exponential factor χ, which is small if $b \ll \lambda$. The anisotropy is pronounced when δ_m is large, which can be achieved by using thicker FM layers and decreasing the density of the superconducting electrons. The ratio δ_m is temperature-dependent and eventually decreases when temperature decreases starting from the SC transition temperature T_s. However, at the temperature of vortex disappearance $T_v < T_s$, the value of the FM film renormalized magnetization $\tilde{m}$ becomes zero and χ again becomes exponentially small. Thus anisotropy has a minimum between T_v and T_s.

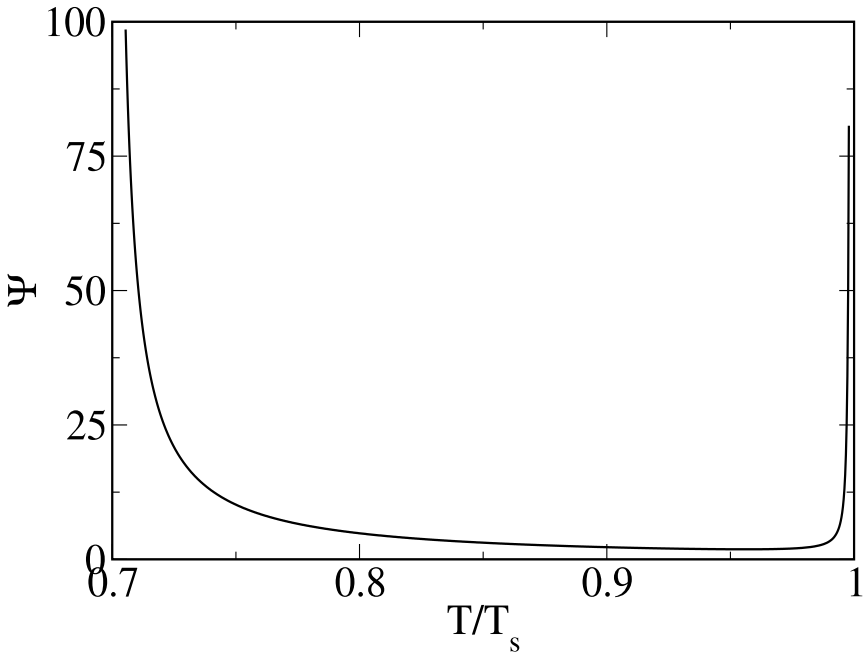

Fig. 17. The ratio $J_c^{||}/J_c^{\perp}$ as a function of temperature with the temperature is in the range $T_v \leq T \leq T_s$.

To study the dependence of the transport anisotropy on temperature T, I define

the ratio Ψ of the parallel critical current $J_c^{||}$ to the perpendicular current $J_c^{\perp}$

$$\Psi = \frac{\phi_0}{\tilde{m}(T)a\chi(T)} \tag{3.30}$$

Recall that in $3D$ superconductor the electron density behaves with temperature as $n_s(T) = n_s(T=0)(1-T^2/T_s^2)$, while $\lambda_L(T) = \lambda_L(T=0)(1-T^2/T_s^2)^{-1/2}$ and $\xi(T) = \xi(T=0)(1-T^2/T_s^2)^{-1/2}$. In $3D$ the Ginzburg-Landau parameter is independent of temperature, so $\kappa_{3D}(T) = \kappa_{3D}(T=0)$, but in thin films the effective penetration depth is $\lambda = \lambda_L^2(T)/d_s$, so $\kappa_{2D}(T) = \kappa_{2D}(T=0)(1-T^2/T_s^2)^{-1/2}$. The vortex disappearance temperature T_v depends on the $2D$ magnetization of the FM film and is determined by setting $\tilde{m}(T=T_v) = 0$. The dependence of parallel to perpendicular critical current on temperature is depicted in Fig.17.

Kopnin and Vinokur [34] considered a collection of superconducting grains with the washboard pinning potential as a model for random pinning. They obtained a similar result for vortex sliding in an external magnetic field with a supercurrent applied. In contrast to their work (they considered vortices only), I consider vortices and antivortices in a periodic pinning field and completely neglect the random pinning.

Now, I briefly discuss how the magnetic field generated by the supercurrent changes the results obtained in this work. In [35] [36] it was shown that at sufficiently small critical magnetic field the domains vanish. Therefore, in general, a magnetic field suppresses both the anisotropy and periodic pinning at a critical field for which domains disappear. At such a critical field only random pinning prevails. However, the total current per unit length is proportional to the thickness of the SC film and can be kept small.

In conclusion, I studied the transport properties of the FM-SC bilayer in a state with stripe domains of alternating magnetization and vorticity. In the absence of a driving force, the vortices and antivortices are arranged in a straight chain configu-

ration. The force between two chains of vortices falls off exponentially as a function of the distance separating the chains. I argued that, in the vicinity of the superconducting transition temperature T_s and the vortex disappearance temperature T_v, the distances between chains becomes much larger than the distance between vortices in the same chain. I solved the equations of motion for vortices and antivortices for the driving current direction parallel and perpendicular to the domains. The parallel critical current is much higher than the perpendicular one, at least in a vicinity of the two transition temperatures. This strong transport anisotropy is due to the fact that, for perpendicular current, the induced motion is a Goldstone mode specific to a system of mobile domains and vortices. I expect the ratio of the parallel to perpendicular critical current to be in the range $10^2 \div 10^4$ close to the superconducting transition temperature T_s and to the vortex disappearance temperature T_v. The anisotropy decreases rapidly when the temperature goes from the ends of this interval, reaching a minimum somewhere inside it. The anisotropy can be destroyed by a rather weak magnetic field perpendicular to the bilayer. This anisotropic transport behavior might serve as a diagnostic tool to discover spontaneous topological structures in magnetic-superconducting systems.

CHAPTER IV

CONCLUSION

This dissertation focuses on the statics and dynamics of the spontaneous vortex phase in heterogeneous ferromagnetic-superconducting systems. In particular, it considers the interaction between a superconducting thin film covered by ferromagnetic textures such as a magnetic dot with in-plane magnetization, an elliptical magnetic dot, a circular magnetic annulus and a finite ferromagnetic rod. For each case, I calculated the magnetic field distributions, screening currents, and total energy of the system. It also analyzes the pinning forces and studies the dynamical properties of ferromagnetic-superconducting bilayers.

In chapter one a brief introduction is given. Chapter two is divided into five sections. The first section discusses the general formulation of HFSS within the London approximation. Section two considers the interaction between an ferromagnetic dot with in-plane magnetization placed on the of an SC thin film. The vector potential and magnetic field produced by the FM were calculated. I calculated the total energy of the system and showed that the spontaneous creation of vortex-antivortex pairs becomes energy favorable when the magnetization of the dot exceeds a threshold value. The phase transitions from a fluxless regime to regimes with one or two vortex-antivortex pairs were studied. In section three, I study the influence of the dot's geometry on the spontaneous vortex phase induced by the dot itself by considering the interaction of vortices in a thin SC film with an elliptical FM dot. I calculated the magnetic fields, screening currents and energy of the system and studied phase transitions from a phase without vortices to phases with one or more vortices. I compared between the results for an elliptic dot with those derived for a circular dot that has the same $2D$-magnetization and the same area as its elliptic counterpart. It is

shown that the elliptical dot is more efficient to induce a spontaneous vortex phase in the superconductor.

The fourth section considers the interaction of vortices in a SC thin film with a circular FM dot of radius R_2 that has a hole of radius R_1 at its center to form a circular annulus. The magnetization of the annulus is assumed to be along the normal to SC film. It was shown that spontaneous vortex creation in the superconductor becomes energy favorable if the annulus's magnetization exceeds a critical value. I calculated the energy of a system of a vortex coupled to the annulus and showed that the equilibrium position for the center of the vortex lies on a circle of radius $R_1 < \rho_0 < R_2$. The degeneracy of the of the vortex location can be eliminated by creating other holes in the dot or moving the hole from the center of the dot. Identical holes located at equal distance from the center of the dot generate identical pinning potentials for the vortices in the SC. Such a setup could be used for quantum computing [19] in a way similar to that discussed by Ioffe and Feigelman [37]. Another opportunity is to use an elliptical annulus instead of circular one. In the case of elliptical annulus, the circle of minimum energy configuration disappear and two minima point will appear instead. The system of elliptical annulus is another possibility for quantum computing setup. In section five, I studied the interaction between an FM columnar defect penetrating an SC thin film. The interaction between the FM and SC vortices strongly alters the pinning potential found by Mkrtchyan and Schmidt [23] in their work on the interaction between vortices and non magnetic cavities in the SC. The vortex is exactly pinned at the center of the rod. Spontaneous creation of vortices by the rod is possible and the phase transition from the vortexless phase to another with one vortex bound to the rod is studied numerically.

Chapter three studies the transport properties of ferromagnetic-superconducting bilayers [38] assuming the stripe domain structure of alternating magnetization and

vorticity. I analyzed pinning forces in this system and showed that the pinning force along the domains is much less that the one perpendicular to the domains. The parallel pinning forces are temperature dependent and they are small enough at temperatures close to the SC transition temperature T_s. The critical current values for two different directions for driving force either parallel or perpendicular to the domains were calculated. A comparison between the critical current for parallel driving and perpendicular driving showed that the system displays a finite resistance if the current is perpendicular to the domains and it is superconducting for parallel current. The dependence of the perpendicular to parallel critical current on temperature is determined. The ratio of the parallel to perpendicular critical current becomes very large in the vicinity of T_s and the vortex disappearance temperature T_v while it has a minimum in the range between T_s and T_v.

The coexistence of ferromagnetism and superconductivity in HFSS offers a new mechanism for vortex pinning. The origin of vortex pinning in the systems I considered here is the inhomogeneous distribution of fields. If the magnetization of the texture is large enough then the strong interaction between the FM and the SC not only can pin vortices but also spontaneously create them in the superconductor. The interaction between the FM and SC is temperature dependent and it is strongest in the vicinity of the SC transition temperature T_s. Pinning forces in ferromagnetic superconducting bilayer are highly anisotropic, the anisotropy of pinning forces reflects itself in different critical current for different driving angle. Such anisotropic transport properties may be used as a diagnostic tool to discover new topological defects. I conclude that the coexistence of superconductivity and ferromagnetism allows for stronger pinning of vortices in the superconductor; therefore, enhancing the critical current of the superconductor. The geometry and magnetization distribution of the FM characterize the properties of the static and dynamical phases of

the superconductor.

REFERENCES

[1] L. Civale, A. D. Marwick, T. K. Worthington, M. A. Kirk, J. R. Thompson, L. Krusin-Elbaum, Y. Sun, J. R. Clem, and F. Holtzberg, Phys. Rev. Lett. **67**, 648 (1991).

[2] G. Blatter, M. V. Feigel'man, V. B. Geshkenbein, A. I. Larkin and V. M. Vinokur, Rev. Mod. Phys. **66**, 1125 (1994).

[3] M. Baert, V. V. Metlushko, R. Jonckheere, V. V. Moshchalkov, and Y. Bruynseraede, Phys. Rev. Lett. **74**, 3269 (1995).

[4] Y. Nozaki, Y. Otani, K. Runge, H. Miyajima, B. Pannetier, J. P. Nozieres, and G. Fillion, J. Phys. **79**, 8571 (1996).

[5] P. Martinoli, M. Nsabimana, G.A. Racine, H. Beck, and R. Clem, Helv.Phys.Acta **56**, 765 (1983).

[6] J. I. Martin, M. Velez, J. Nogues, and I. K. Schuller, Phys. Rev. Lett. **79**, 1929, (1997).

[7] D. J. Morgan and J. B. Ketterson, Phys. Rev. Lett. **80**, 3614(1998).

[8] M. J. Van Bael, J. Bekaert, K. Temst, L. Van Look, V. V. Moshchalkov, Y. Bruynseraede, G. D. Howells, A. N. Grigorenko, S. J. Bending, G. Borghs, Phys. Rev. Lett. **86**, 155 (2001).

[9] M. Lange, M. J. Van Bael, L. Van Look, K. Temst, J. Swerts, G. Guntherodt, V. V. Moshchalkov, Y. Bruynseraede, Europhys. Lett. **51**, 110 (2001).

[10] S. J. Bending, G. D. Howells, A. N. Grigorenko, M. J. Van Bael, J. Bekaert, K. Temst, L. Van Look, V. V. Moshchalkov, Y. Bruynseraede, G. Borghs, R. G. Humphreys, Physica C**332**, 20 (2000);

[11] V. L. Ginzburg, Zh. E'ksp. Teor. Fiz. **31**, 202 (1957) [Sov. Phys. JETP **4**, 153 (1957)].

[12] I. F. Lyuksyutov and V. L. Pokrovsky Phys. Rev. Lett. **81**, 2344 (1998).

[13] I. F. Lyuksyutov and V. L. Pokrovsky, cond-mat/9903312.

[14] M. J. Van Bael, K. Temst, V. V. Moshchalkov, Y. Bruynseraede, Phys. Rev. B **59**, 14674 (1999).

[15] L. N. Bulaevskii, A. I. Buzdin, M. L. Kulic and S. V. Panyukov, Adv.Phys. **34**, 175 (1985).

[16] S. Erdin, M. A. Kayali, I. F. Lyuksyutov and V. L. Pokrovsky, Phys. Rev. B **66**, 014414 (2002).

[17] I. K. Marmorkos, A. Matulis and F. M. Peeters Phys. Rev. B **53**, 2677 (1996).

[18] M. A. Kayali, Phys. Lett. A **298**, 432 (2002).

[19] M. V. Milosevic and F. M. Peeters, Phys. Rev. B**68**, 094510 (2003).

[20] S. Erdin, I. Lyuksyutov, V. Pokrovsky and V. Vinokur, Phys. Rev. Lett. **88**, 017001 (2002).

[21] R. Sasik, T. Hwa, cond-mat/0003462.

[22] M. A. Kayali, Phys. Rev. B **69**, 012505 (2004).

[23] G. S. Mkrtchyan and V. V. Schmidt, Sov. Phys. **JETP** 34 (1972) 195.

[24] J. Pearl, J. Appl. Phys. Lett. **5**, 65 (1964).

[25] P. G. de Gennes, *Superconductivity of Metals and Alloys* (Addison-Wesley, New York, 1989).

[26] A. A. Abrikosov, *Introduction to the Theory of Metals* (North-Holland, Amsterdam, 1986).

[27] I. S. Gradshteyn and I. M. Ryzhik, *Table of Integrals, Series, and Products* (Academic Press, Boston,1994), 5th ed.

[28] A. Buzdin, M. Daumens, Physica C **294**, 257 (1998).

[29] A. Buzdin, D. Feinberg, Physica C **256**, 303 (1996).

[30] C. Meyers, M. Daumens, and A. Buzdin, Physica C **325**, 118 (1999).

[31] A. Buzdin, M. Daumens, Physica C **332**, 108 (2000).

[32] C. Meyers, A. Buzdin, Phys. Rev. B **62**, 9762 (2000).

[33] J. Bardeen and M. J. Stephen, Phys. Rev. **A 140**, 1197 (1965).

[34] N. B. Kopnin and V. M. Vinokur, Phys. Rev. Lett. **83**, 4864 (1999).

[35] Ar. Abanov, V. Kalatsky, V. L. Pokrovsky and W. Saslow, Phys. Rev. **B 51**, 1023 (1995)

[36] A. P. Malozemoff and J. C. Slonczewski, *Magnetic Domain Walls in Bubble Materials* (Academic Press, New York, 1979).

[37] L. B. Ioffe and M. V. Feigel'man, Phys. Rev. B **66**, 224503 (2002).

[38] M. A. Kayali and V. L. Pokrovsky, Phys. Rev. B **69**, 018413 (2004).

APPENDIX A

GLOSSARY OF ACRONYMS

CD: Columnar Defect.

EMD: Elliptical Magnetic Dot.

FM: Ferromagnet or Ferromagnetic.

FSB: Ferromagnetic Superconducting Bilayer.

HFSS: Heterogeneous Ferromagnetic Superconducting Systems.

SC: Superconductor or Superconducting

SV: Superconducting Vortex.

VITA

M. Amin Kayali was born in Aleppo, Syria, on February 27, 1970. He obtained his B.S. in physics and mathematics in 1993 from University of Aleppo, Aleppo, Syria. After graduation, he spent a year in the high energy physics group at the International Center for Theoretical Physics, Trieste, Italy. In 1994 he joined the graduate program at Cambridge University, Cambridge, UK and in 1995 he obtained a M.S. in mathematics. Afterward, he returned back to the University of Aleppo where he worked there as a research associate in theoretical physics until 1997 when he left to Oxford University, Oxford, UK to work as a research fellow in the mathematical science department. Since 1998, he has been pursuing his M.S. and Ph.D. studies in physics at Texas A & M University. He will continue his research as a postdoctoral fellow at the Human Neuroimaging Laboratory, Baylor College of Medicine, One Baylor Plaza, Room S104, Houston, Texas 77030.

The typist for this thesis was Mohammad Amin Kayali.